NAVAL POSTGRADUATE SCHOOL
Monterey, California

Step Frequency High PRF Waveform Design

by

G.S. Gill
Paulo A. Soares

DTIC QUALITY INSPECTED 3

June 1996

19961015 017

Approved for public release; distribution is unlimited.

Naval Postgraduate School
Monterey, California 93943-5000

Rear Admiral M. J. Evans
Superintendent

R. Elster
Provost

This work was prepared for NRaD, NCCOSC, San Diego, CA 92152-5000.

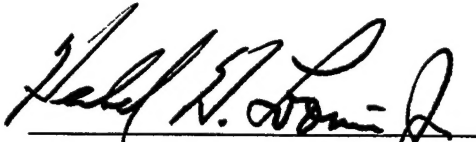Approved for public release; distribution is unlimited.

This report was prepared by:

G. S. GILL
Visiting Assoc. Professor
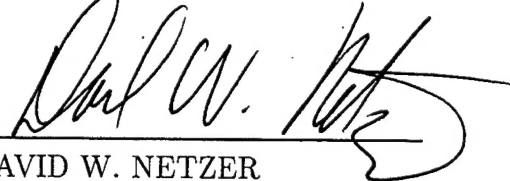Department of Electrical and
Computer Engineering

Reviewed by:

HERSCHEL H. LOOMIS, JR.
Chairman,
Department of Electrical and
Computer Engineering

Released by:

DAVID W. NETZER
Associate Provost and
Dean of Research

REPORT DOCUMENTATION PAGE

Form Approved
OMB No. 0704-0188

Public reporting burden for the collection of information is estimated to average 1 hour per response, including the time for reviewing instructions, searching existing data sources, gathering and maintaining the data needed, and completing and reviewing the collection of information. Send comments regarding this burden estimate or any other aspect of this collection of information, including suggestions for reducing this burden to Washington Headquarters Services, Directorate for Information Operations and Reports, 1215 Jefferson Davis Highway, Suite 1204, Arlington VA 22202-4302, and to the Office of Management and Budget, Paperwork Reduction Project (0704-0188), Washington DC 20503.

1. AGENCY USE ONLY (Leave blank)	2. REPORT DATE June 1996	3. REPORT TYPE AND DATES COVERED Technical Report 1 Jan 96-30 Sep 96

4. TITLE AND SUBTITLE
Step Frequency High PRF Waveform Design

5. FUNDING NUMBERS

6. AUTHOR(S)
G. S. Gill and Paulo A. Soares

7. PERFORMING ORGANIZATION NAME(S) AND ADDRESS(ES)
Naval Postgraduate School
Monterey, CA 93943-5000

8. PERFORMING ORGANIZATION REPORT NUMBER
NPS-EC-96-008

9. SPONSORING/MONITORING AGENCY NAME(S) AND ADDRESS(ES)
Research, Development, Test and Evaluation Division (NRaD)
Naval Command, Control and Ocean Surveillance Center (NCCOSC)
71 Catalina Blvd.
San Diego, CA 92152-5000

10. SPONSORING/MONITORING AGENCY REPORT NUMBER

11. SUPPLEMENTARY NOTES
The views expressed in this report are those of the author and do not reflect the official policy or position of the Department of Defense or the United States Government.

12a. DISTRIBUTION/AVAILABILITY STATEMENT
Approved for public release; distribution is unlimited.

12b. DISTRIBUTION CODE

13. ABSTRACT (Maximum 200 words)

This report discusses the design and analysis of a step frequency waveform for a surface based radar to detect small targets embedded in clutter. Detection of small targets requires significant reduction in clutter which can be achieved with high range resolution radar with narrow range cell size and Doppler processing. High range resolution with conventional constant frequency waveforms requires high speed A/D with large dynamic range, which is limited by existing A/D technology. However, step frequency allows high resolution with modest A/D requirements. The design of a step frequency waveform is complex due to the conflicting effect of waveform parameters on performance goals. In this report, the design process which determines the waveform parameters for given radar specifications, is systemized. A graphical as well as a computer implementation of the design process is presented. The step frequency waveform is analyzed using the ambiguity function which brings out the characteristics and advantages of the waveform. The ambiguity surface and related diagrams are plotted for specific waveforms of interest.

14. SUBJECT TERMS
Step frequency, waveform design, high PRF, high resolution

15. NUMBER OF PAGES
98

16. PRICE CODE

17. SECURITY CLASSIFICATION OF REPORT UNCLASSIFIED	18. SECURITY CLASSIFICATION OF REPORT UNCLASSIFIED	19. SECURITY CLASSIFICATION OF ABSTRACT UNCLASSIFIED	20. LIMITATION OF ABSTRACT SAR

ABSTRACT

This report discusses the design and analysis of a step frequency waveform for a surface based radar to detect small targets embedded in clutter. Detection of small targets requires significant reduction in clutter which can be achieved with high range resolution radar with narrow range cell size and doppler processing. High range resolution with conventional constant frequency waveforms requires high speed A/D with large dynamic range, which is limited by existing A/D technology. However, step frequency allows high resolution with modest A/D requirements. The design of a step frequency waveform is complex due to the conflicting effect of waveform parameters on performance goals. In this report, the design process which determines the waveform parameters for given radar specifications, is systematized. A graphical as well as a computer implementation of the design process is presented. The step frequency waveform is analyzed using the ambiguity function which brings out the characteristics and advantages of the waveform. The ambiguity surface and related diagrams are plotted for specific waveforms of interest.

TABLE OF CONTENTS

I. INTRODUCTION

High range resolution has many advantages in radar. Apart from providing the ability to resolve closed spaced targets in range, it improves the range accuracy, reduces the amount of clutter within the resolution cell, reduces multipath, provides high resolution range profiles and aids in target classification. Typical waveforms for achieving high resolution are ultra wideband (UWB), conventional pulse compression and step frequency waveforms. In all three waveforms, high range resolution is obtained by increased bandwidth. In the first two waveforms large bandwidth is instantaneous, whereas in the step frequency waveform large bandwidth is achieved sequentially over many pulses while keeping the instantaneous bandwidth low. This results in lowering of A/D sampling rate for the step frequency waveform. This is a significant advantage as limitation of A/D technology is a bottleneck in the implementation of high resolution radar.

The use of a step frequency waveform for detailed RCS measurements in anechoic chambers or in open ranges is well known. In these applications, the step frequency waveform along with ISAR processing provides high resolution mapping of rotating targets. The use of the step frequency waveform for operational applications needs to be explored. The purpose of this report is to design the step frequency waveform for detection of small targets embedded in clutter. Any solution to this challenging radar problem would include large improvements in signal-to-noise (S/N) and signal-to-clutter (S/C) ratios. S/N ratio is improved by having large average transmit power or integrating large number of pulses or some combination of both. S/C ratio is improved by reduction of clutter which is achieved in two steps, that is, first by limiting the amount of clutter entering the radar receiver, and secondly by canceling the clutter in doppler processing. The amount of clutter entering the

1

radar receiver is achieved by decreasing the effective pulse width which is normally done with a conventional pulse compression waveform to keep adequate S/N ratio.

It should be noted that conventional constant frequency medium or high PRF waveforms would satisfy the above requirements for large improvement in S/N and S/C ratios. However, the constant frequency waveforms would require high speed A/D's to achieve small range cell size. High PRF waveforms will be highly ambiguous in range and the range ambiguities will further increase the clutter problem as clutter from various range zones due to different pulses arrive simultaneously to compete with the target signal. To accommodate the large folded clutter, A/D would require a large dynamic range and high sampling rate, a combination difficult to achieve in practice. Thus, requirements for systems with fine range resolution may not be met with the existing A/D technology. Step frequency can alleviate the A/D problem by easing the requirements both on the sampling rate and the dynamic range.

Range resolution in step frequency is controlled by frequency spread over the pulse burst (which is $N\Delta f$, where N is the number of pulses in the burst and Δf is the frequency step) but the sampling rate depends upon the pulse width. Thus, in the step frequency radar sampling rate is made independent of the range resolution which allows lowering its value without sacrificing range resolution. The dynamic range in step frequency radar is reduced by limiting the folded clutter from ambiguous ranges. Unlike constant frequency radars, multiple time around clutter in step frequency radar does not come from the entire range extent but is limited by the number of frequency lines which will pass through the IF filter. The number of frequency lines and thus the number of ambiguous range zones is $1/\tau\Delta f$ (where τ is the pulse width). With judicious choice of waveform parameters it is possible to limit the

2

dynamic range of the clutter as well as the sampling rate of A/D and still meet the high resolution requirements.

The design of constant frequency waveforms is relatively simple and well documented. However, the design of step frequency waveforms is complex due to the conflicting effect of waveform parameters on various desired performance goals. Thus, in this report effort is made to systematize the design process for the high PRF step frequency waveform. The goals in the design of a high PRF waveform include keeping the target in clutter free area, keeping the target doppler unambiguous and meeting other radar performance specifications.

Also, use is made of the ambiguity function to determine the characteristics and special advantages of the step frequency waveform. Finally, ambiguity diagrams are sketched for a specific waveform of interest.

4

II. INTRODUCTION TO THE STEP FREQUENCY RADAR

This chapter gives a brief introduction to the concepts and implementation of the step frequency radar before the discussion of the waveform design, which is done in the next chapter.

A. STEP FREQUENCY WAVEFORM

The step frequency waveform consists of a series of N pulses each with a pulse width of τ, and whose frequency is increased from pulse to pulse in steps of Δf, as shown in Figure 1. The frequency of the nth transmitted pulse is given by

$$f_n = f_0 + (n-1)\Delta f, \tag{2.1}$$

where f_0 is the nominal carrier frequency, Δf is the frequency step size and $n = 1, 2, 3, ..., N$.

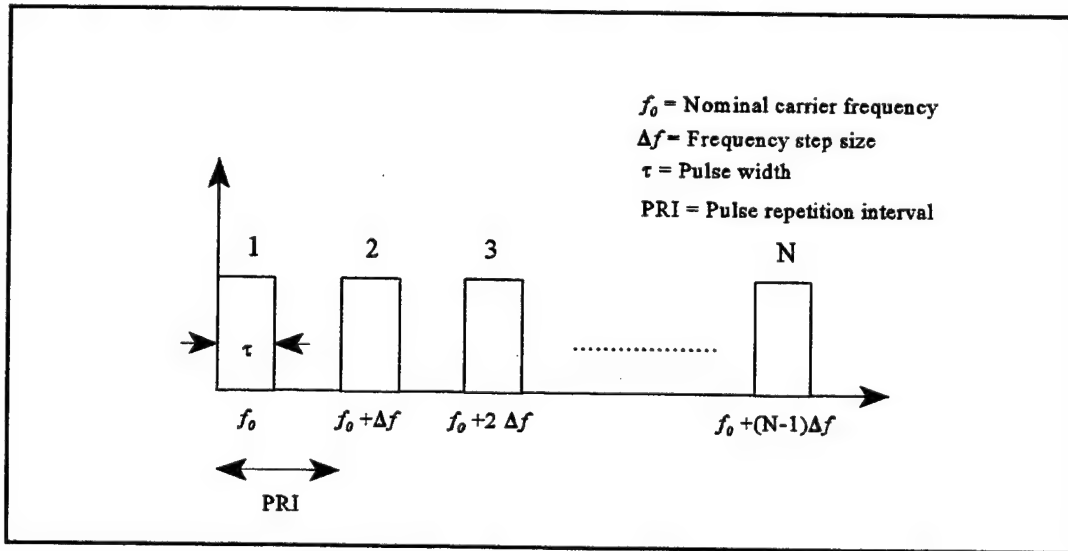Figure 1.   Step Frequency Waveform.

Although the instantaneous bandwidth of a step frequency waveform is approximately $1/\tau$, a much larger effective bandwidth can be achieved. This effective bandwidth is given by

$$B_{eff} = N\Delta f. \tag{2.2}$$

The range resolution for this waveform is not the conventional value of $c\tau/2$. The synthetic range resolution obtained by coherently processing a series of N returns from the target, can be much smaller and is given by

$$\Delta R = \frac{c}{2B_{eff}} = \frac{c}{2N\Delta f}, \tag{2.3}$$

where c is the speed of light (3×10^8m/sec). The fact that in the step frequency radar, resolution does not depend on the instantaneous bandwidth and the fact that resolution can be increased arbitrarily by increasing $N\Delta f$, are significant advantages. There is a constraint on selection of Δf (i.e., $\Delta f \leq 1/\tau$), however, N can be increased to achieve high range resolution.

B. SYSTEM DESCRIPTION AND IMPLEMENTATION

The implementation of the step frequency radar is similar to the coherent Pulse-Doppler radar. The system implementation can be observed in Figure 2. The core of the system is a coherent step frequency synthesizer with an output frequency called f_{syn}, which is stepped from pulse to pulse by a fixed step size, Δf. Therefore, we can write

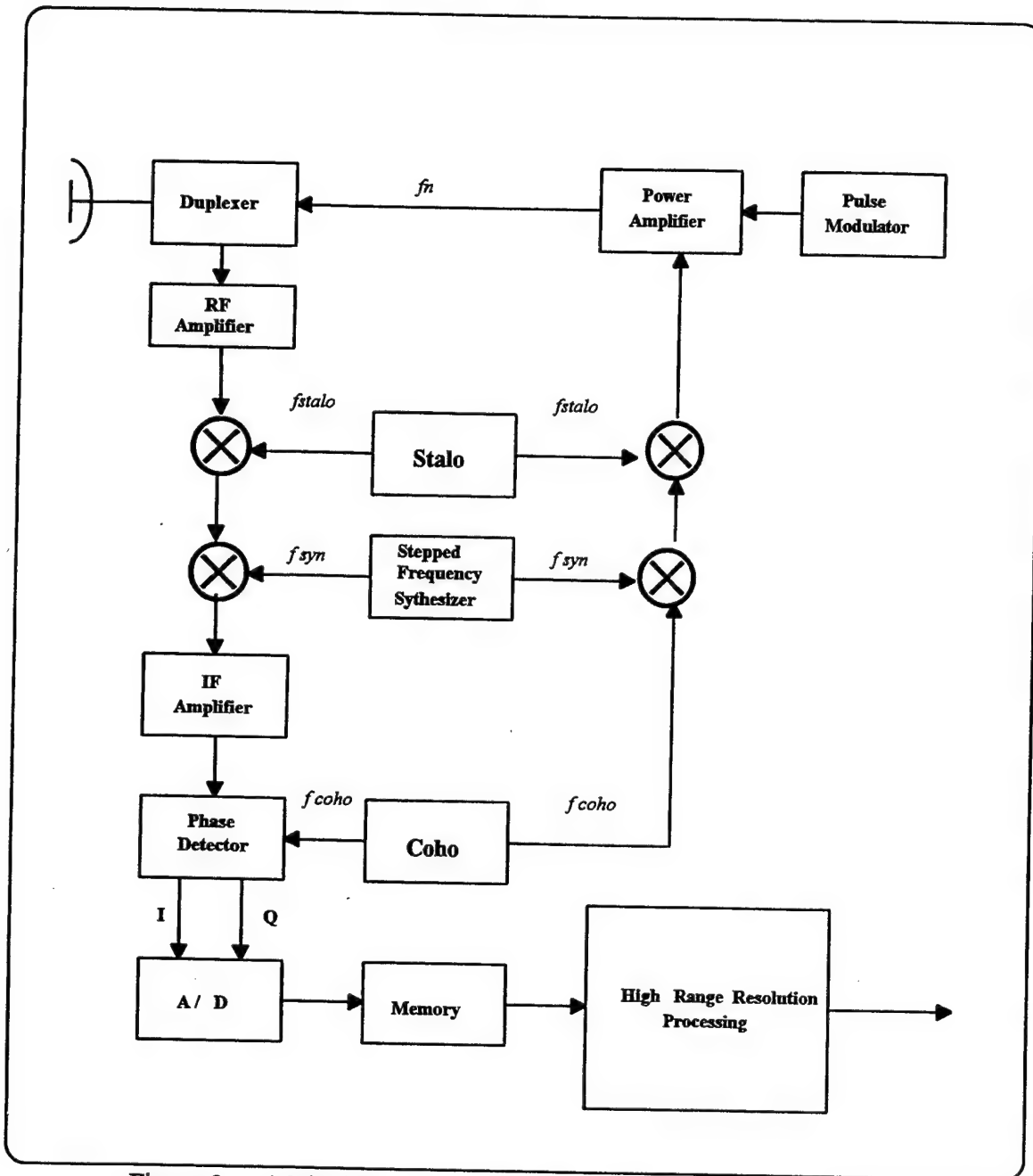$$f_{syn} = (n-1)\Delta f. \tag{2.4}$$

6

Figure 2. A Block Diagram of the Stepped-Frequency Radar.

The frequency of a local coherent oscillator (COHO), f_{coho}, is first mixed with the output frequency of the step frequency synthesizer, f_{syn}. Then the sum frequency is converted to the final transmitted frequency by mixing it with the frequency of the stable local oscillator (STALO), f_{stalo}. The sum frequency of this second mixer is then pulse modulated and amplified before the transmission occurs. Each transmitted pulse will have a carrier frequency comprised of three different components: the fixed IF frequency, f_{coho}, the fixed RF frequency, f_{stalo}, and the variable frequency of the stepped frequency synthesizer, f_{syn}. Thus, the carrier frequency of the nth pulse is given by the following equation:

$$f_n = f_{stalo} + f_{coho} + f_{syn} = f_0 + (n-1)\Delta f. \qquad (2.5)$$

In the receiver side, the return signal is first down converted by mixing it with f_{stalo}. The resulting signal is further down converted to intermediate frequency (IF) by mixing with f_{syn}. The output signal obtained after the second mixer is the IF signal. The signal is then divided into two different channels, the in-phase channel (I), and the quadrature channel (Q). Both, the in-phase and the quadrature signals are mixed with the output signal of the coherent oscillator. The first is mixed directly and the second is mixed with the COHO signal after this last one has been shifted 90 degrees. The I and Q components, both in the video frequency range, are sampled by an A/D converter at a rate equal to the inverse of the pulse width.

Each complex sample is usually called *range bin*, thus range bin may be defined as a memory location for temporary storage of successive pairs of numbers representing the I and Q samples of the radar return received at a given point in the interpulse period. A separate

bin therefore must be provided for each sampling interval (range gate). To the extent that range is unambiguous, the numbers stored in any one bin represent successive returns from a single range increment, hence the name range bin. Because of the correspondence of the range bins to the sampling intervals (when A/D conversion follows I and Q detection), range bin has come to be used synonymously with *sampling interval* as well as *range gate*.

Sampled returns from incoming pulses are stored im memory until all the pulses within the same burst have been received and can be processed as shown in Figure 3. Figure 4 describes the organization of sample storage in memory. Complex samples for each range bin are transformed by taking the FFT of samples in each range bin, resulting in a high resolution range profile (HRR profile).

One important advantage of the step frequency radar compared with other radars which also use wideband waveforms, is that in the former the narrow instantaneous bandwidth does not require a high analog to digital sampling rate which can be a major limitation in the system design. On the other hand, the step frequency radar may require more complex signal processing.
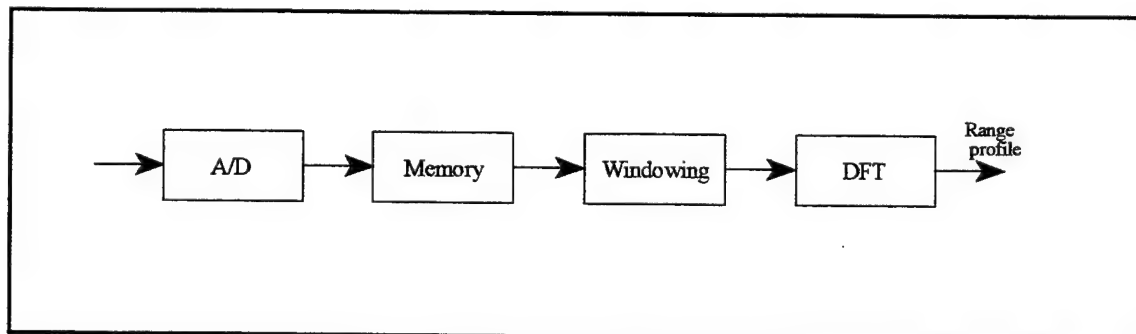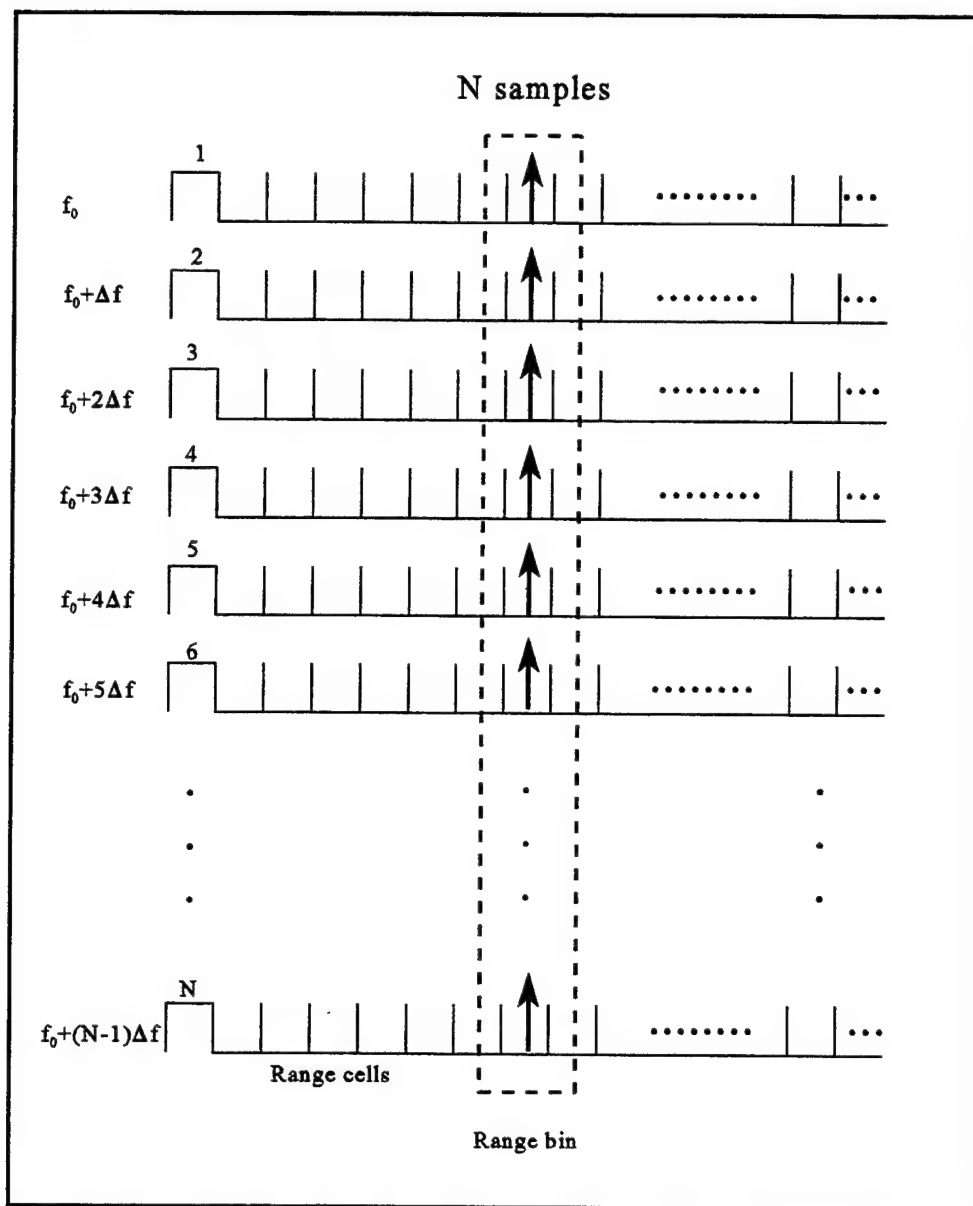

Figure 3. Elementary processing.

Figure 4. N samples from a target are collected and stored in memory for processing.

C. WAVEFORM PROCESSING

The radar return signal at the output of the coherent detector can be written as

$$s(n) = I(n) + jQ(n) = A_n \exp(j\phi_n), \tag{2.6}$$

where

A_n = the magnitude of the nth pulse;

ϕ_n = the phase of the nth pulse.

A_n represents an amplitude factor which depends on the transmitted power, the size of the target, and other factors in radar range equation.

The phase of the nth pulse can be written as

$$\phi_n = 2\pi f_n t_r = 2\pi f_n \frac{2R_n}{c}, \tag{2.7}$$

where f_n is the carrier frequency of the nth pulse and t_r is the round trip time from the target measured by the nth pulse. This time is equal to $2R_n/c$, with R_n being the range between the target and the radar. For a target with constant velocity toward the radar, the range R_n is given by

$$R_n = R_0 - (n-1)vT, \tag{2.8}$$

where

R_0 = initial target range;

T = pulse repetition interval;

v = relative radial velocity between target and radar.

11

The overall expression for the baseband return signal can now be determined by substituting the instantaneous frequency from Equation 2.1, and the target range from Equation 2.8 in Equation 2.7, and then substituting the resulting expression in Equation 2.6. The resulting equation is as follows:

$$s(n) = A_n \exp\left[j \frac{4\pi}{c} f_n R_n\right]$$

$$= A_n \exp\left[j \frac{4\pi}{c} \left(f_0 + (n-1)\Delta f\right) \left(R_0 - (n-1)vT\right)\right] .$$

(2.9)

Equation 2.9 can be rewritten as

$$s(n) = A_n \exp\left[\frac{4\pi f_0 R_0}{c} + 2\pi \frac{\Delta f}{T} \frac{2R_0}{c}(n-1)T + 2\pi \frac{2vf_0}{c}(n-1)T + 2\pi \frac{2v(n-1)\Delta f}{c}(n-1)T\right].$$

(2.10)

The first term represents a constant phase shift which is not of any practical significance. The second term is the multiplication of the rate of change of frequency $\Delta f/T$ with the round trip time $2R_0/c$. This term represents a shift in frequency during the round trip time $2R_0/c$. Thus the range (or the round trip time) is converted into a frequency shift (which is analogous to conversion of range to frequency in linear frequency modulated CW radar). Therefore, it is possible to resolve and measure the range by resolving the frequency, which can be done by taking the DFT of the received signal from N frequency stepped pulses. Since the range is measured by taking the DFT, the range measurement will have the same limitations as the frequency measurement by DFT. Thus, the range resolution ΔR and

unambiguous range R_u are dependent on the frequency resolution and the maximum unambiguous frequency measurement by DFT, respectively. This range resolution of $c/2N\Delta f$ is equivalent to the resolution obtained by conventional pulse compression with a compression ratio of $N\tau\Delta f$. The maximum value of the compression ratio is limited to N for practical cases (as $\tau\Delta f$ is constrained to be equal to or less than unity). For detection of moving targets, range resolution can be traded off for creation of clear space within the range window R_u. The third term in Equation 2.10 represents the doppler frequency shift due to target motion and it adds to the frequency shift of the second term. The range resolution process unwillingly treats the doppler frequency as a frequency shift due to range and thus results in shifting of target range from its true range. The fourth term in Equation 2.10 is due to the interaction of the changing frequency of the step frequency waveform with the target motion. The doppler shift changes with each pulse (even for constant velocity targets) because of the change in pulse frequency. The doppler shift due to the constant frequency component f_0 has already been taken into account in the third term. The fourth term gives the doppler shift $2vn\Delta f/c$ due to the frequency step of the nth pulse. Thus, the return from a moving target due to N frequencies will contain N frequency components in the data domain instead of ideally containing one component. This spread in frequency of $2Nv\Delta f/c$ when processed by DFT will lead to a spread in range by vNT, which in terms of range bins is given by

$$P = \frac{vNT}{\Delta R} = \frac{2vN^2T\Delta f}{c} .$$

(2.11)

13

III. STEP FREQUENCY WAVEFORM DESIGN

Radar waveforms can be classified as low PRF, high PRF or medium PRF. A low PRF is, by definition, one for which the maximum range the radar is designed to handle lies in the first range zone - the zone from which first-time-around echoes are received. Range for low PRF is unambiguous and doppler frequency is ambiguous. A high PRF is one for which the observed doppler frequencies of all significant targets are unambiguous and range is ambiguous. Finally, a medium PRF is one for which neither of these conditions is satisfied. Both range and doppler frequency are ambiguous. In this report the interest is in the high PRF waveform.

The purpose of this chapter is to develop a design procedure for detection of small targets with a surface (land or sea) based step frequency radar which employs a high PRF waveform. The disadvantage of high PRF is that the range ambiguity has to be resolved. However, several advantages result from high PRF. The unambiguous doppler leads to advantages such as elimination of clutter and absence or minimization of the blind doppler problem. It also improves the signal-to-noise (S/N) ratio by integration of larger number of pulses. For a constant frequency high PRF waveform, multiple time around clutter (from ambiguous regions due to different pulses) adds up and thus decreases the signal-to-clutter (S/C) ratio and increases the dynamic range of the receiver and associated A/D. Though the S/C ratio can be improved by doppler filtering, receiver and A/D will still require a large dynamic range as a large magnitude of folded clutter has to be accommodated in the receiver and A/D. The step frequency waveform reduces the folded clutter and thus the dynamic range by decreasing the number of range ambiguities. Range ambiguities in the step frequency

15

waveform depend upon the number of pulses which will pass through the IF filter simultaneously. This number is given by $1/(\tau\Delta f)$. By proper choice of the product $\tau\Delta f$, range ambiguities and thus clutter and dynamic range can be reduced. However, this advantage comes about at the cost of limiting the range coverage. This feature of the step frequency waveform provides a good tradeoff as high resolution radars are often limited by A/D technology. The waveform design involves the selection of PRF (f_r), number of pulses (N), frequency step (Δf) and pulse width (τ). It is assumed that the following radar performance related parameters are available: range resolution (ΔR), nominal carrier frequency (f_0), time-on-target (tot), minimum and maximum radial velocity (v_{min} and v_{max}) and the maximum number of pulses (N_{max}). The design of constant frequency waveforms is relatively simple and well documented. However, the design of step frequency waveforms is complex due to the conflicting effect of waveform parameters on various desired performance goals. Thus, in this report effort is made to systematize the design process for the high PRF step frequency waveform. The main point behind the design of high PRF waveforms is to keep the target in clutter free area and the target doppler unambiguous. This involves selection of PRF based on minimum and maximum target velocities and other parameters. PRF should be large enough that target at maximum expected velocity stays unambiguous in doppler. The other constraint is based on the fact that target doppler from minimum target velocity exceeds the clutter doppler. These constrains along with resolution requirements lead to the high PRF waveform design.

In this chapter, the method used to compute the desired parameters for the high PRF design case will be explained, but first two parameters will be defined and the expression for constraints on PRF will be derived.

1.   Definition of two constants

A dimensionless parameter P that relates the radial target motion over the time duration of the step frequency waveform to the resolution of the profile can be defined as:

$$P = \frac{vNT}{\Delta R},$$ (3.1)

where:

v = the radial velocity between the radar and the target (closing velocity);

NT = the duration of the step frequency waveform;

ΔR = the processed range resolution.

This is the ratio of how far the target moved with respect to the range resolution cell during the integration time. For all velocities with magnitude greater than zero, this represents a mismatch in the DFT (which acts like a matched filter), resulting in attenuation and dispersion of the HRR profile. In addition to the attenuation and dispersion that will result in a reduction in range resolution and S/N ratio, the uncompensated radial velocity will shift the HRR profiles by L FFT bins, where L is given by:

$$L = \frac{f_0}{B} P,$$ (3.2)

where:

f_0 = the nominal transmitter frequency (center frequency);

B = the total processed bandwidth.

2. Derivation of PRF constraints

To get a moving target in clutter free zone after DFT processing, the motion induced doppler shift should be such that shift L exceeds the clutter extent,

$$L \geq N\tau\Delta f. \qquad (3.3)$$

From Equations 3.1, 3.2 and 3.3

$$\frac{2NTv}{\lambda} \geq N\tau\Delta f. \qquad (3.4)$$

From above v_{min} is obtained as

$$
\begin{aligned}
v_{min} &= \frac{\lambda}{2T}\tau\Delta f \\
&= \frac{\lambda}{2T}\tau\frac{c}{2N\Delta R} \qquad (3.5)\\
&= \frac{\lambda}{2T}\frac{c\tau}{2N}\frac{1}{\Delta R}.
\end{aligned}
$$

The constraint for maximum velocity can be derived by considering the worst case scenario for a target located at the end of the range gate (of width $c\tau/2$) at the maximum speed. To keep the doppler unambiguous, doppler shift and spread together should not exceed the PRF and therefore

$$L+P < N - N\tau\Delta f. \qquad (3.6)$$

Substituting the value of L and P into this last equation,

$$\frac{2NTv}{\lambda} + \frac{vNT}{\Delta R} < N(1-\tau\Delta f)$$

$$\frac{2Tv}{\lambda} + \frac{vT}{\Delta R} < 1-\tau\Delta f \qquad (3.7)$$

$$v + \frac{vT}{\Delta R}\frac{\lambda}{2T} < \frac{\lambda}{2T} - \tau\Delta f\frac{\lambda}{2T} \ .$$

Last term in right hand side of above equation can be recognized as the minimum velocity from Equation 3.5 and therefore

$$v\left(1+\frac{\lambda}{2\Delta R}\right) < \frac{\lambda}{2T} - v_{min}$$

$$v_{max}\left(1+\frac{\lambda}{2\Delta R}\right) + v_{min} \le \frac{\lambda}{2T} = \frac{\lambda}{2}f_r \ . \qquad (3.8)$$

Now, solving for f_r:

$$f_r \ge \frac{2}{\lambda}\left[v_{max}\left(1+\frac{\lambda}{2\Delta R}\right) + v_{min}\right]. \qquad (3.9)$$

Equality will give the minimum PRF ($f_{r\,min}$). If the factor $\lambda/(2\Delta R) \ll 1$, then the previous equation can be reduced to

$$f_r \ge \frac{2}{\lambda}\left[v_{max} + v_{min}\right]. \qquad (3.10)$$

3. Design Method

The initial specifications are the nominal carrier frequency (f_0), range resolution (ΔR), maximum radial velocity (v_{max}), minimum radial velocity (v_{min}), time on target (*tot*) and due

19

to processing constraints, the maximum number of pulses (N_{max}). The waveform parameters that we want to calculate are the PRF (f_r), number of pulses (N), frequency step size (Δf) and the pulse width (τ).

The proposed method consists of five steps, as follows:

1. Selection of PRF from given equation . This equation gives the minimum PRF and the exact value can be determined using an iterative procedure later.

2. The number of pulses is determined from *tot* and f_r :

$$N \geq (tot) f_r = \left(\frac{\theta_B}{\dot{\theta}_S} \right) f_r, \tag{3.11}$$

where θ_B is the antenna beamwidth and $\dot{\theta}_S$ is the scan rate.

3. The frequency step size is calculated from

$$\Delta f = \frac{c}{2 N \Delta R}, \tag{3.12}$$

where c is the speed of light (3×10^8 m/sec).

4. The pulse width is chosen from Equation 3.5, which can be rewritten as

$$\tau \leq \frac{2}{\lambda} \frac{v_{min}}{f_r \Delta f}. \tag{3.13}$$

N and τ will impact the S/N ratio which determines the radar performance, that is probability of detection and probability of false alarm for given radar parameters. Therefore it should be ascertained from the following equation that chosen N and τ yield adequate S/N

ratio to satisfy the radar performance requirements.

$$\frac{S}{N} = \frac{P_t G^2 \lambda^2 \sigma (\tau N)}{(4\pi)^3 R^4 k T_0 F L},$$ (3.14)

where

P_t = the transmitted peak power (watts);

G = the antenna gain of the transmitter/receiver;

λ = the wavelength (meters);

σ = the radar cross section of the target (square meters);

τ = the pulse width (meters);

N = the number of pulses coherently integrated within one scan;

R = the detection range of the target (meters);

k = Boltzmann's constant (1.38×10^{-23} watt-second/°K);

T_0 = the noise temperature (°K);

F = the receiver noise figure;

L = a loss factor incorporating all system losses.

By convention, T_0 is taken to be 290°K, which is close to room temperature (300°K)

and conveniently makes the product kT_0 a round number (4×10^{-21} watt-second/°K).

5. Flexibility in PRF constraint can be used to satisfy other design objectives such as

the search range;

$$Search\ range\ =\ number\ of\ R_u\text{'s}\ .\ R_u$$

$$=\ \frac{B_{IF}}{\Delta f}\ R_u$$

$$=\ \frac{k/\tau}{\Delta f}\ R_u \qquad (3.15)$$

$$=\ \frac{k}{\tau \Delta f}\ \frac{c}{2\Delta f}.$$

where R_u is the unambiguous range and B_{IF} is the intermediate frequency bandwidth. $N, f_r,\ \tau$ and Δf are changed iteratively such that the required search range is obtained. Extent of R_u should not increase clutter as range resolution is already fixed. However the number of $R_u\text{'s}$ will increase clutter (which should not matter if cancellation is adequate).

The initial specifications and the final calculated design parameters can be summarized in the following table:

Specifications	Calculated Design Parameters
Range resolution (ΔR)	Minimum PRF (f_r)
Nominal carrier frequency (f_0)	Number of pulses (N)
Time-on-target (tot)	Frequency step size (Δf)
Minimum radial velocity (v_{min})	Pulse width (τ)
Maximum radial velocity (v_{max})	
Maximum number of pulses (N_{max})	

Table 1. Summary of specifications and design parameters.

4. Graphical implementation of the Design Method

Using the equations mentioned in the previous section, a graphical method to design the waveform was developed. The first graph is a plot of the range resolution versus minimum PRF, for four different nominal carrier frequencies.
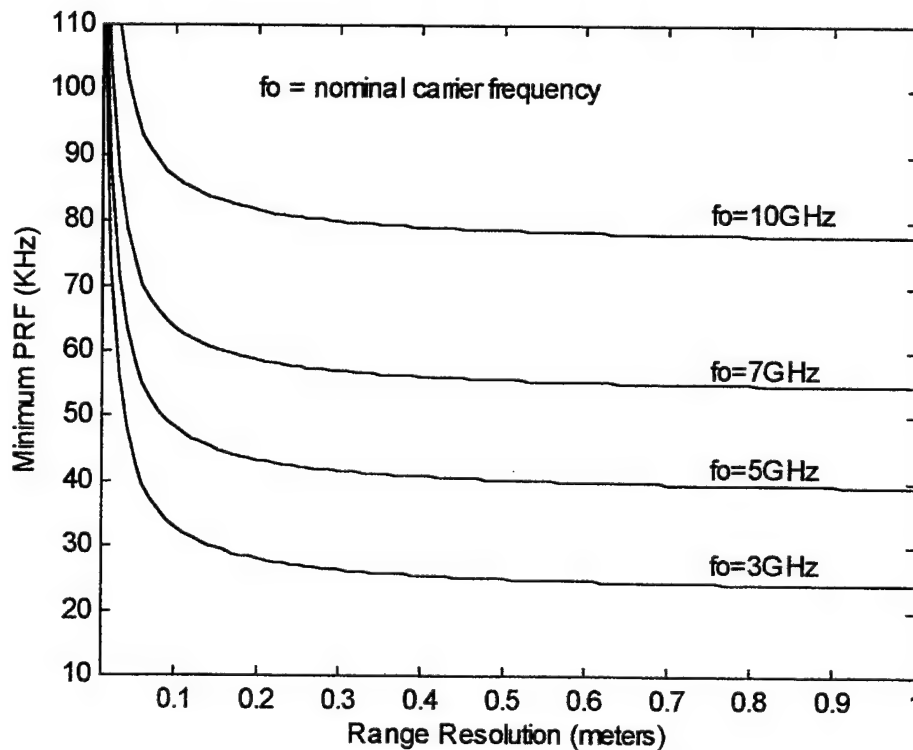

Figure 5. Minimum PRF versus range resolution for four different nominal carrier frequencies.

This graph was created using Equation 3.9 and it can be observed that as the value of the desired range resolution decreases (corresponding to an improvement in the range resolution), the minimum PRF increases. This graph is used to determine the PRF for a given range resolution and carrier frequency.

The next graph, Figure 6, is a plot of the PRF versus the number of pulses, and was generated using Equation 3.11.
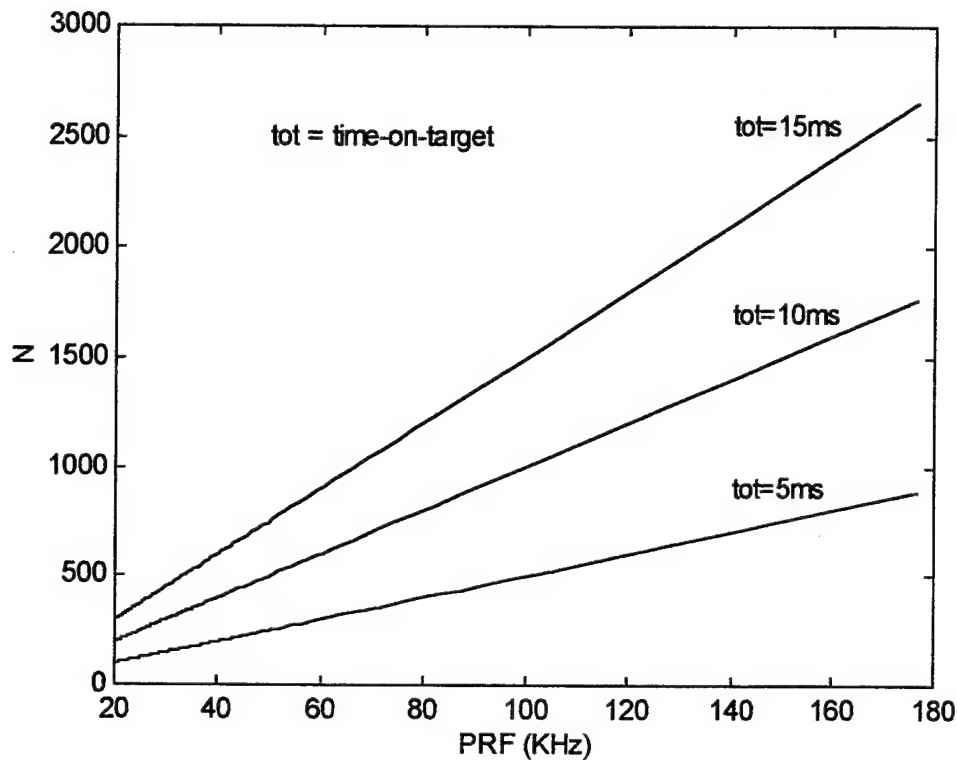

Figure 6. Number of pulses versus PRF for three different times-on-target (5, 10, and 15 ms).

This plot is used to determine the number of pulses for a given time-on-target (tot) and PRF, computed in the previous step from Figure 5. Then, and using Equation 3.12, the frequency step size was plotted versus the number of pulses, for three different values of range resolution (0.3, 0.5, and 1 meter) as can be observed in Figure 7. This graph is used to determine the frequency step for a given range resolution and number of pulses computed in the previous step from Figure 6. The frequency step size required for the same number of

24

pulses increases as the desired range resolution decreases. Therefore, the better range resolution is desired, the higher the frequency step size must be.
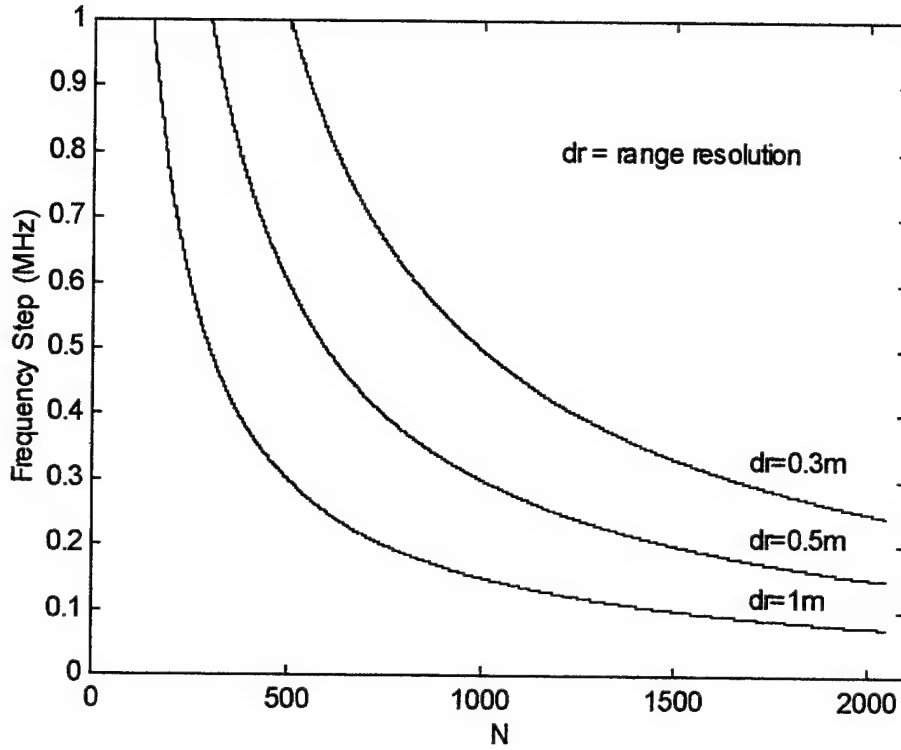

Figure 7.   Frequency step versus number of pulses for three different range resolutions (0.3, 0.5, and 1 meter).

Finally, the last step is to compute the pulse width using Equation 3.13, and all the calculated design parameters from Table 1 will be obtained.

Note that in all the calculations and plots above described v_{min} was considered to be 150 m/s and v_{max}, 1000 m/s. The value considered for N_{max} was 2048.

Consider an example to determine the design parameters for a step frequency radar with a nominal carrier frequency of 10 GHz, time-on-target of 15 ms and a desired range resolution of 0.3 m. From Figure 5 a minimum PRF of 80 KHz would be obtained. Using this

value and Figure 6, N would be approximately equal to 1200. Now with N=1200, dr=0.3m and using Figure 7, the frequency step would be approximately 0.42 MHz. The last step is to compute the value of the pulse width using Equation 3.14 and the result would came up to be τ=298 ns.

Interpolation should be used in this plots whenever the specifications are different from the values in the plots. However some times the desired values are beyond the plotted values. Additionally, not only we want to compute the desired parameters that satisfy the initial specifications, but also we may want to satisfy some parameter constraints. Therefore a MATLAB code was written in order to fulfill this requirement. This program can be found in Appendix B.

5.   Computer implementation of the Design Method

The waveform design parameters are constrained to the following values:

- Pulse width - between 50 nsec and 5000 nsec

- Frequency step - should be 0.4, 0.6, 0.8 or 1 MHz

- PRF - should be an integer multiple of 5 KHz

The program is written in a way so that it will ask for the desired range resolution, nominal carrier frequency, and the time-on-target and these data should be entered from the keyboard. With this input data the program will compute the minimum values using the equations previously presented. These values are iterated until the constraints mentioned above are all satisfied and the desired design parameters obtained. The minimum values are shown in brackets. The program will also compute the actual range resolution and time-on-target corresponding to the rounded values of the PRF, frequency step, pulse width and number of

26

pulses. Figure 8 illustrates how the screen will appear.

Enter the desired range resolution in meters : 0.3

Enter the nominal carrier frequency in GHz : 10

Enter the time-on-target in msec : 15

The calculated design parameters are :   (minimum values)

- PRF = 140.00 KHz   (80.00 KHz)
- Frequency step = 0.40 MHz   (0.42 MHz)
- Pulse width = 180.00 nsec   (300.00 nsec)
- Number of pulses = 2048   (1200)
- Actual range resolution = 0.19 m
- Actual time-on-target = 14.63 msec

Figure 8. Example of the screen when running *program2.m* .

IV. STEP FREQUENCY WAVEFORM ANALYSIS USING THE AMBIGUITY FUNCTION

A. INTRODUCTION

In this chapter, the ambiguity function for a specific step frequency waveform will be determined. The waveform with the following parameters is of practical interest:

$$t_s = 0.1 \ \mu sec,$$

$$T = 5 \ \mu sec,$$

$$\Delta f = 1 \ MHz,$$

$$N = 500,$$

where t_s is the pulse width, T is the PRI, Δf is the frequency step, and N is the number of pulses. However, it is difficult to compute and plot this ambiguity function with the desired resolution because of the very large amount of computations involved. Not only the amount of computations is large but also the plotting is hard to handle because the files can easily reach several megabytes. Therefore, waveforms with parameters similar to the waveform of interest but easier to compute will be investigated, to bring out the key characteristics of the waveform under investigation. First, theoretical dimensions will be verified with a few cases. Then, these theoretical dimensions will be used for particular case of interest which is difficult to compute directly.

Since the ambiguity function of the step frequency waveform contains elements of ambiguity functions of linear frequency modulated (LFM) pulses and train of constant frequency pulses, the ambiguity functions of these waveforms will be introduced along with the general introduction to ambiguity function in Appendix A.

B. AMBIGUITY FUNCTION OF THE STEP FREQUENCY WAVEFORM

The transmitted signal of the step frequency radar (as shown in Figure 1) can be represented mathematically as follows:

$$S_t(t) = A_t \sum_{n=0}^{N-1} s(t-nT) \, e^{j2\pi(f_0+n\Delta f)t} \,, \tag{4.1}$$

with $s(t)$ defined as
$$s(t-nT) = 1, \qquad\qquad \text{if } nT \le t \le nT+t_s \,,$$
$$= 0, \qquad\qquad \text{elsewhere}, \tag{4.2}$$

and $n = 0, \dots, N\text{-}1$. A_t is the amplitude of the transmitted signal. Equation 4.1 can be rewritten as follows:

$$S_t(t) = A_t \left[\sum_{n=0}^{N-1} s(t-nT) \, e^{j2\pi n\Delta f t} \right] e^{j2\pi f_0 t}$$

$$= A_t \, S(t) \, e^{j2\pi f_0 t} \,, \tag{4.3}$$

The expression in brackets is the complex envelope of the pulse sequence represented by $S(t)$.

The received signal can be written as

$$S_r(t) = A_r \, S(t-\tau) \, e^{j2\pi(f_0+f_d)(t-\tau)} \,, \tag{4.4}$$

and the ambiguity function as

$$|\chi(\tau,f_d)| = \left| \int_{-\infty}^{+\infty} \left[\sum_{m=0}^{N-1} s(t-mT) \, e^{j2\pi m\Delta f t} \sum_{n=0}^{N-1} s^*(t-nT-\tau) \, e^{-j2\pi n\Delta f(t-\tau)} \right] e^{2\pi f_d t} \, dt \right| . \tag{4.5}$$

Changing variables ($t-mT = t'$), the final expression for the ambiguity function of the step frequency waveform is obtained:

$$|\chi(\tau, f_d)| = |\sum_{m=0}^{N-1} \sum_{n=0}^{N-1} e^{j2\pi m^2 \Delta f T} e^{j2\pi m f_d T} e^{-j2\pi mn\Delta f T} e^{j2\pi n\Delta f \tau}$$

$$\times \int_{-\infty}^{+\infty} s(t') \, s^*(t'-(n-m)T-\tau) \, e^{j2\pi(m-n)\Delta f t'} \, e^{j2\pi f_d t'} dt' \, | \, . \tag{4.6}$$

The theoretical dimensions of the contours of the ambiguity surface for the step frequency waveform are shown in Figure 9. The overall dimensions are of length 2NT along the delay axis and $2N\Delta f$ along the frequency axis. It can be observed that the distance between component contours along the delay axis is equal to the PRI of the waveform and along the frequency axis is equal to the inverse of the PRI. The ambiguity diagram of the step frequency waveform can be obtained from the ambiguity diagram of the constant frequency pulse train (same parameters), by rotating the delay axis by $\Delta f/T$. This can be stated more accurately by saying that the ambiguity function of the step frequency radar is $\chi(\tau, (\Delta f/T) f_d)$ where $\chi(\tau, f_d)$ is the ambiguity function of the constant frequency pulse train. Apart from rotation of horizontal axis (and all cuts parallel to it) the individual spikes also rotate. This is similar to linear frequency modulation pulses. The extent of the central column of spikes along the frequency axis for zero delay is $2/t_s$, value which decreases when we move away from the center. The central spike as shown in Figure 9 is inclined $\Delta f/T$ with respect to the horizontal axis, indicating the range-doppler coupling of the step frequency waveform. The projection of the central peak on the delay axis is $2t_s$, which is the overall delay uncertainty. However if the doppler is known, the delay uncertainty is given by $2/(N\Delta f)$ as indicated in the figure. The projection of the central peak on the frequency axis is also indicated in the figure. If the
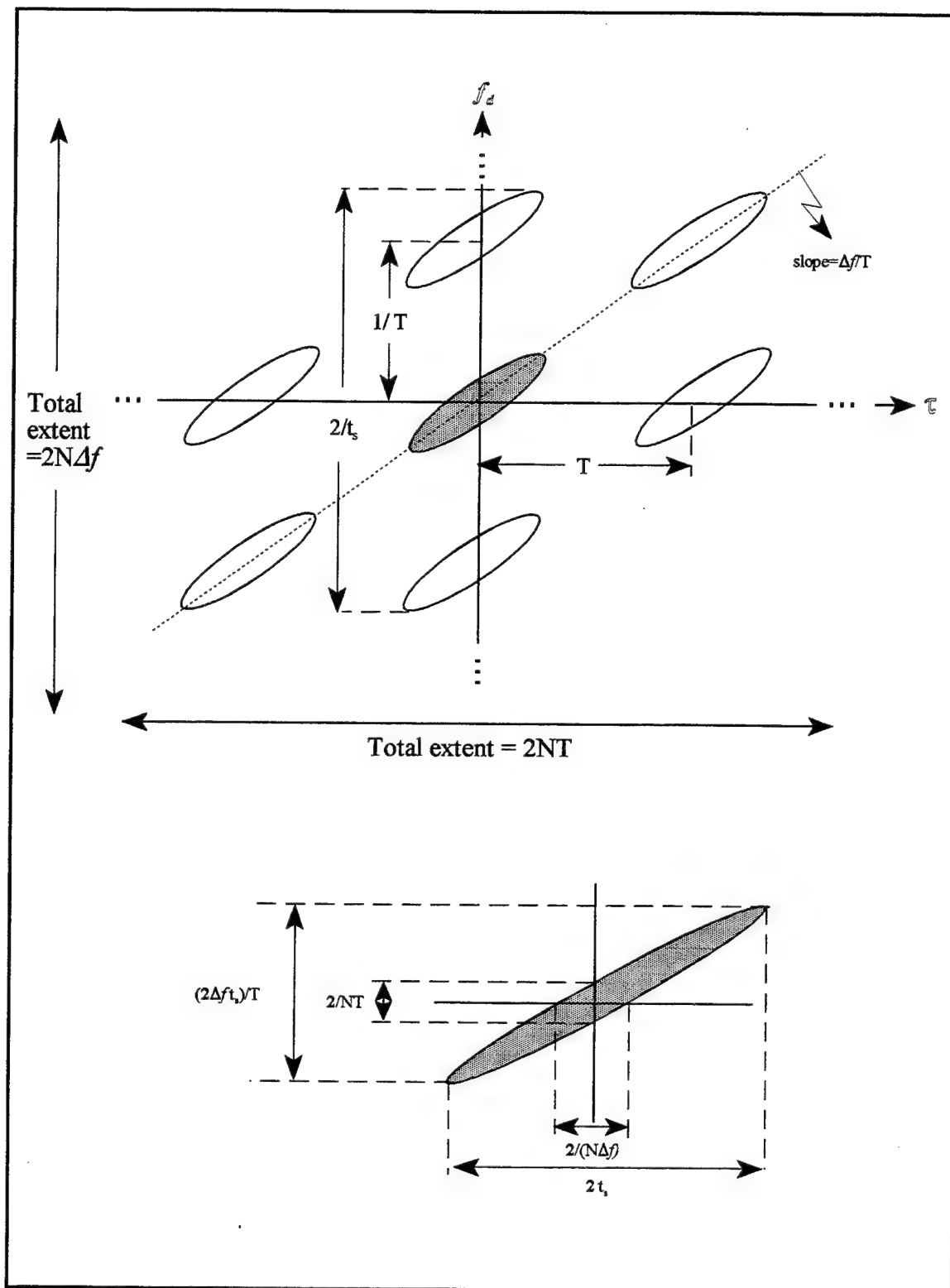
31

Figure 9.   Level contour of the ambiguity surface of a step frequency waveform.

delay is known, the frequency uncertainty is 2/NT which is the same as for the constant frequency pulse train. However if target delay is not known, frequency uncertainty is much larger due to range-doppler coupling.

C. AMBIGUITY FUNCTION OF STEP FREQUENCY WAVEFORMS

Four waveforms will be studied in this section. These waveforms are defined by the following parameters:

1. N=5, t_s =1 μs, PRI =5 μs, Δf =1 MHz.

2. **N=10**, t_s =1 μs, PRI =5 μs, Δf =1 MHz.

3. N=10, t_s **=0.1 μs**, PRI =5 μs, Δf =1 MHz.

4. **N=500**, t_s =0.1 μs, PRI =5 μs, Δf =1 MHz.

1. First waveform

The results for this waveform are shown in Figures 10 through 14. The ambiguity diagram is represented in Figure 10. It can be observed that it is spiky like the one for the constant frequency pulse train, but it is tilted at an angle. The global view of the contour plot of the ambiguity function for this waveform is shown in Figure 11(a). The rotation of the plot with respect to the axes is obvious in the figure and the rotation angle is given by $\Delta f/T$. The delay and frequency axis dimensions match the theoretical values as from -NT to NT and from -NΔf to NΔf. Figure 11(b) is a close up view of the contour plot. Figure 12(a) is a further magnification of the contour plot and Figure 12(b) shows the details of the central peak. From the contour plot it is clear that the central peak is a inclined ridge with the highest magnitude in the center of the contour. Figure 13(a) is a cut of the ambiguity surface along the delay
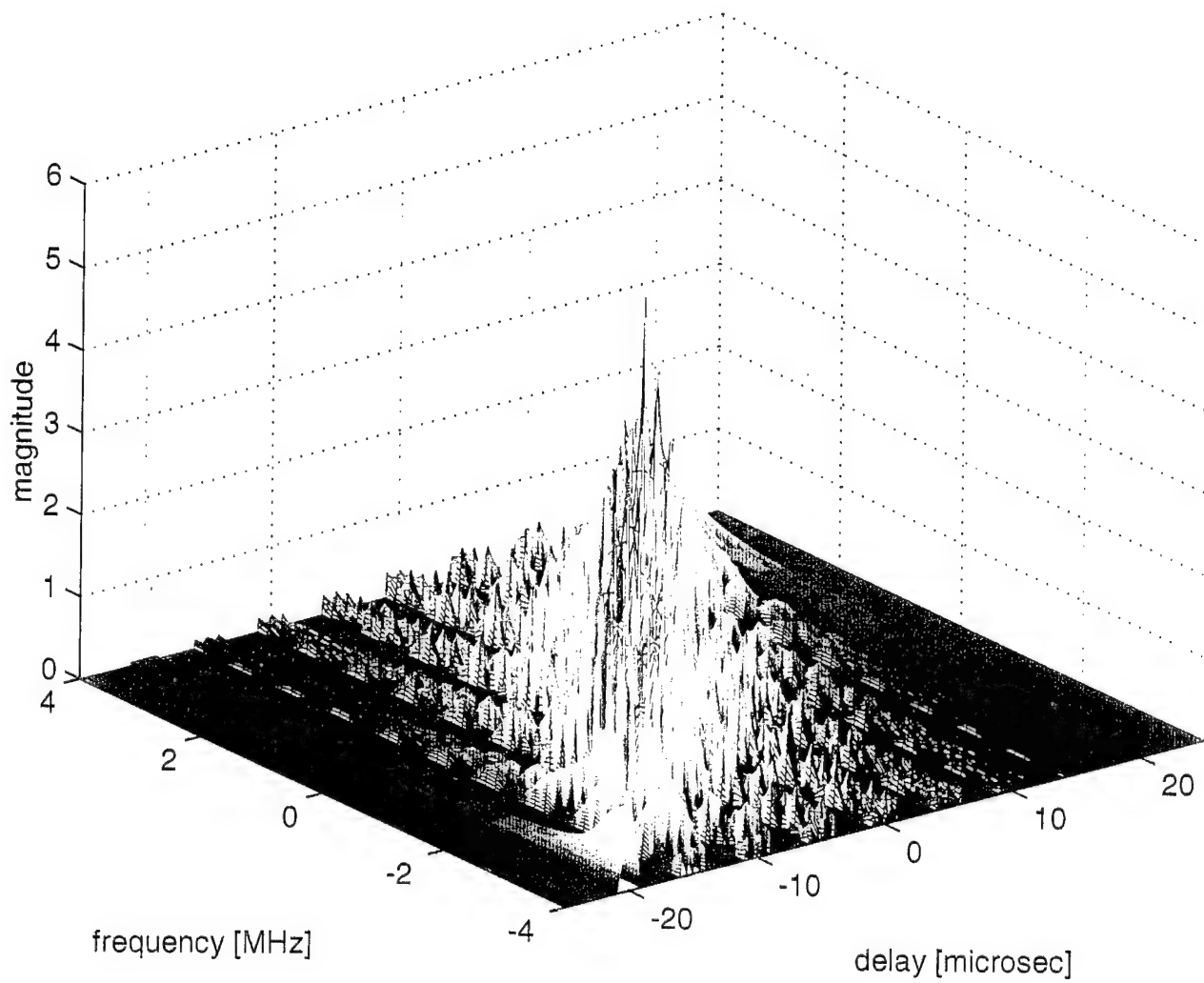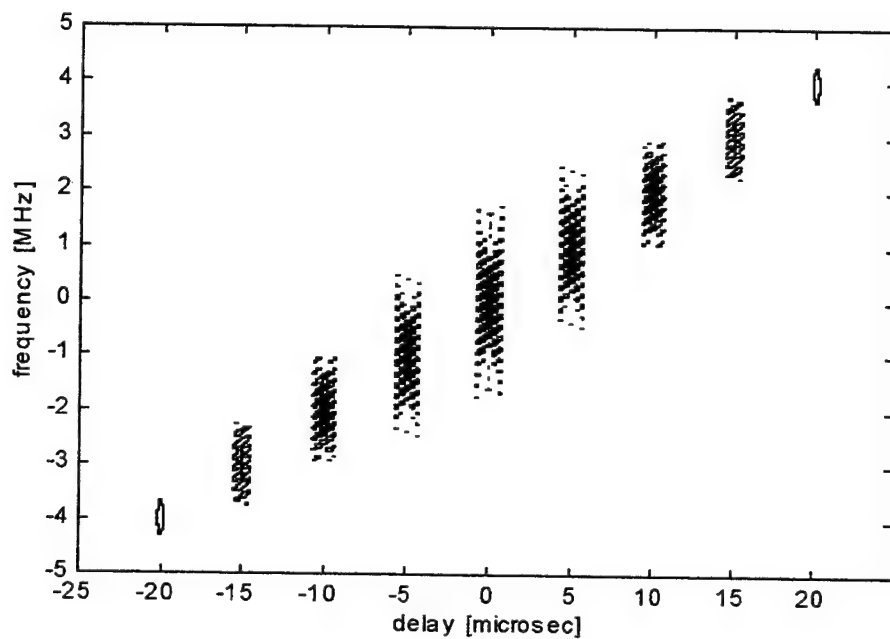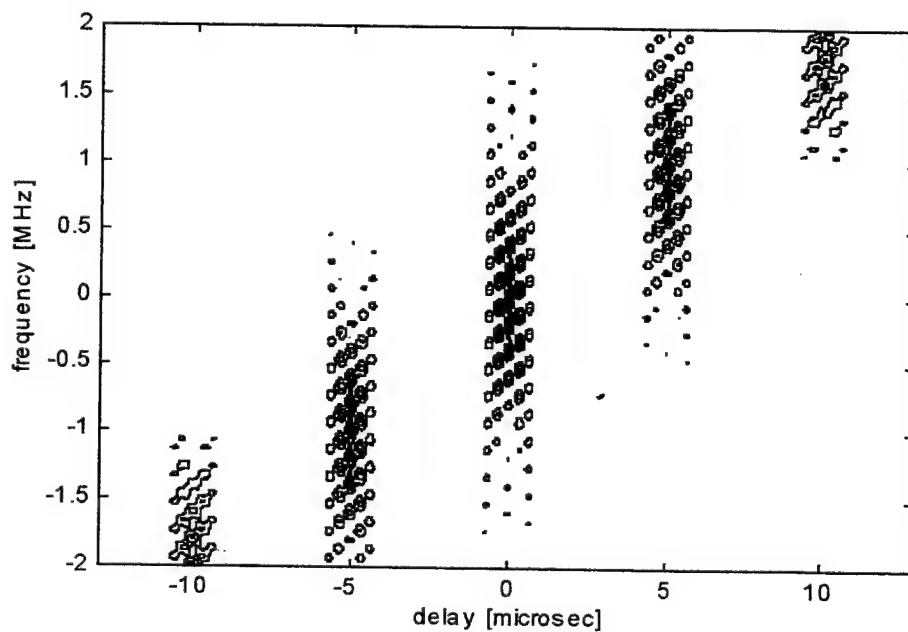
33

Figure 10.   Ambiguity diagram of a step frequency waveform.
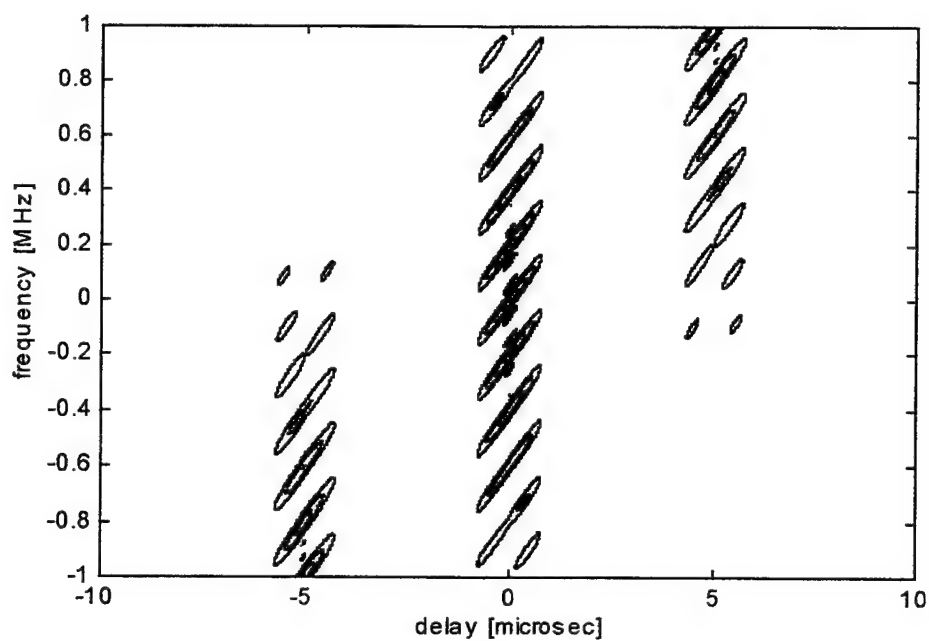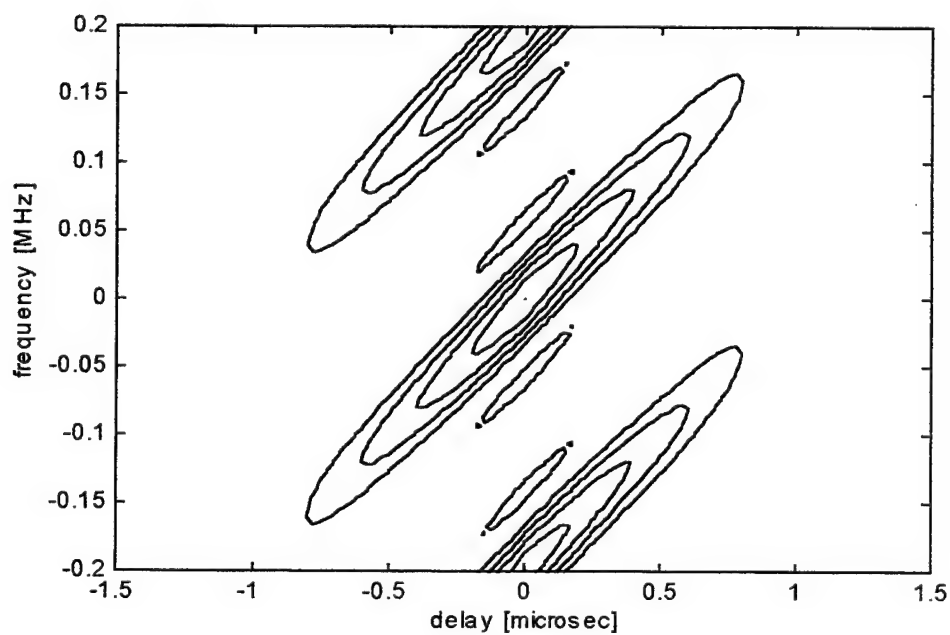
(N=5, pulse width=1 microsec, PRI=5 microsec, Δf=1 MHz)

Figure 11. Contour plots of the ambiguity diagram of a step frequency waveform.
(N=5, pulse width=1 microsec, PRI=5 microsec, Δf=1 MHz)
(a) Global view.
(b) Magnified view.

35

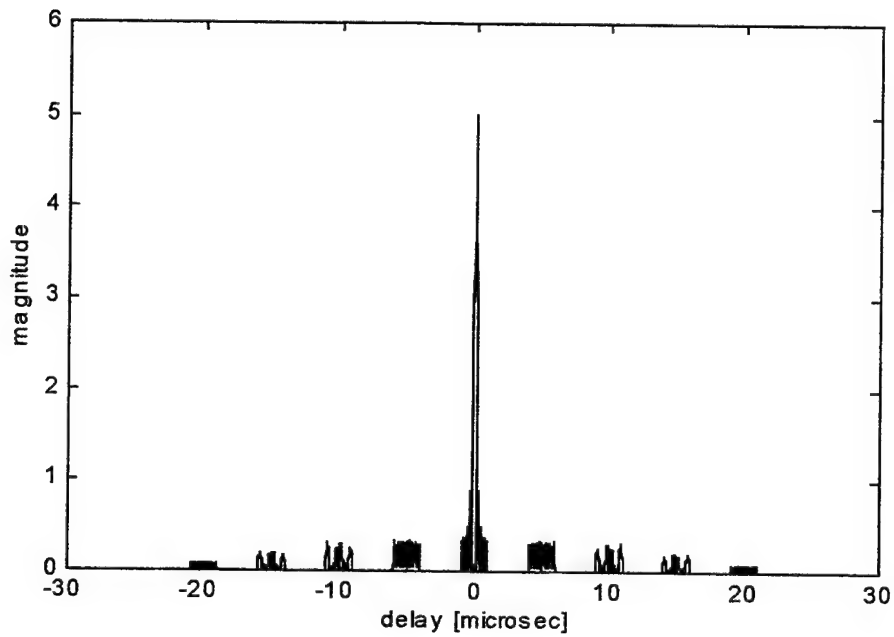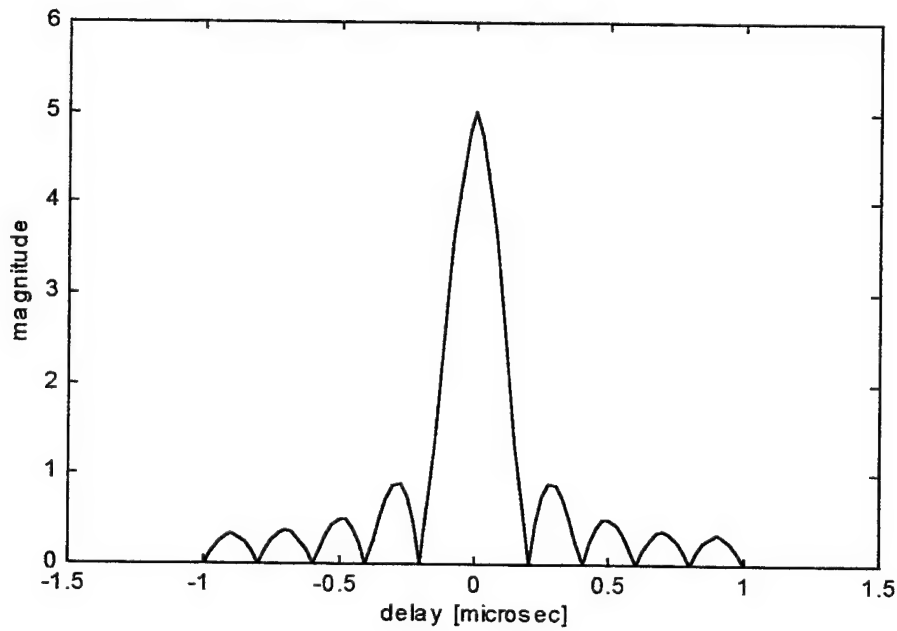Figure 12. Contour plots of the ambiguity diagram of a step frequency waveform.
(N=5, pulse width =1 microsec, PRI=5microsec, Δf=1 MHz)
(a) Magnified view.
(b) Magnified view of the central peak.

(a)

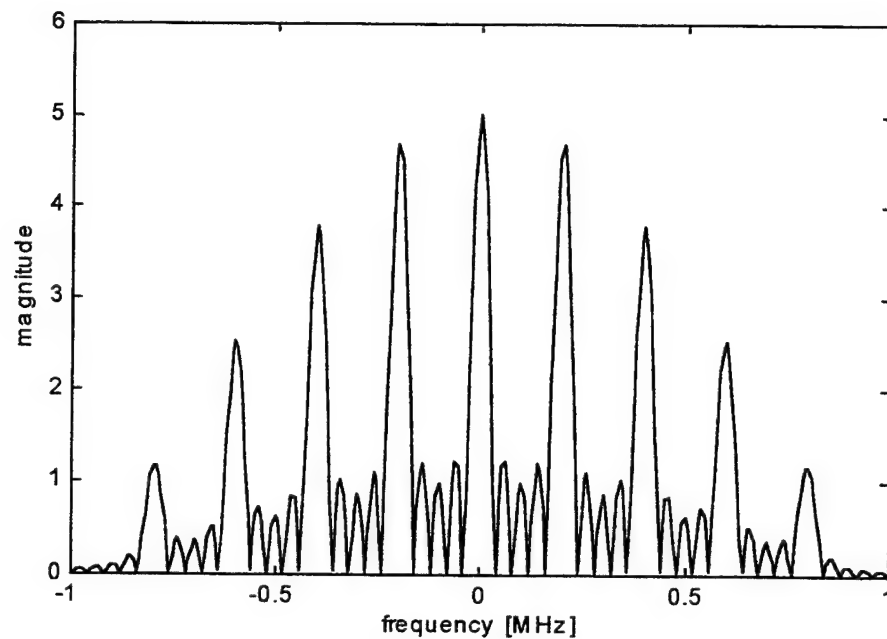

(b)
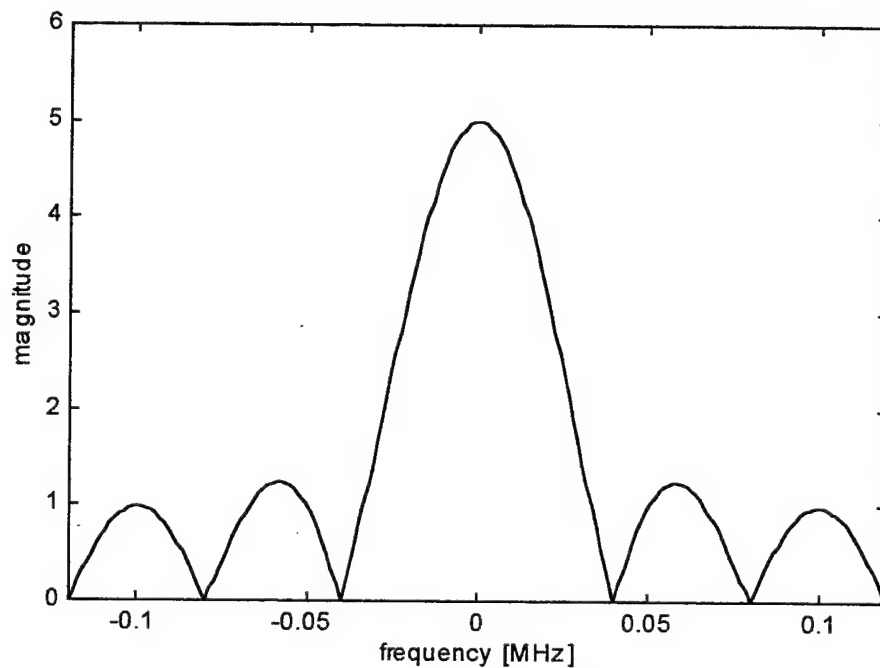
Figure 13. Time profiles of the ambiguity diagram of a step frequency waveform.
(N=5, pulse width =1 microsec, PRI=5 microsec, Δf=1MHz)
(a) Global view.
(b) Magnified view.

(a)

(b)

Figure 14. Frequency profile of the ambiguity diagram of a step frequency waveform.
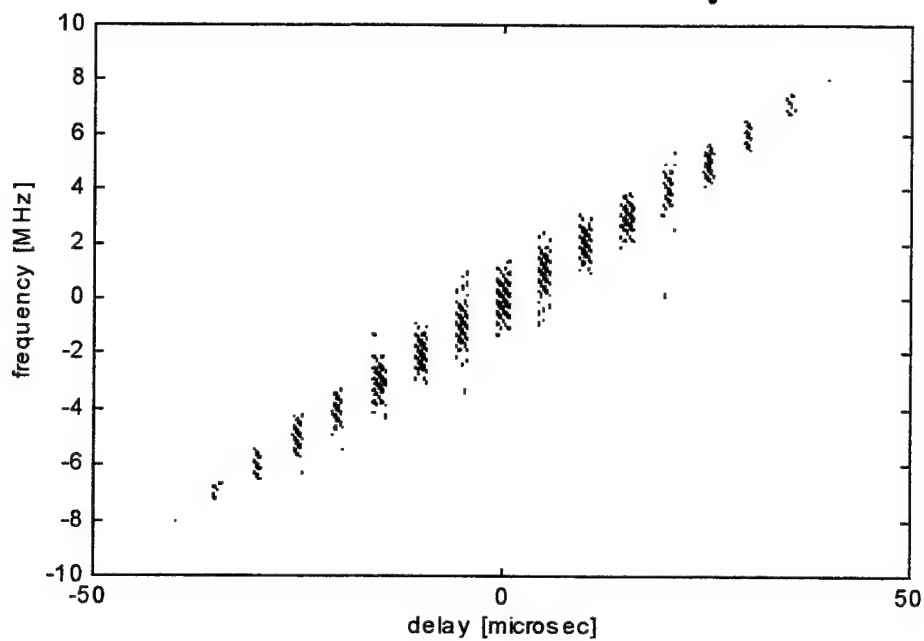(N=5, pulse width =1 microsec, PRI=5 microsec, Δf=1MHz)
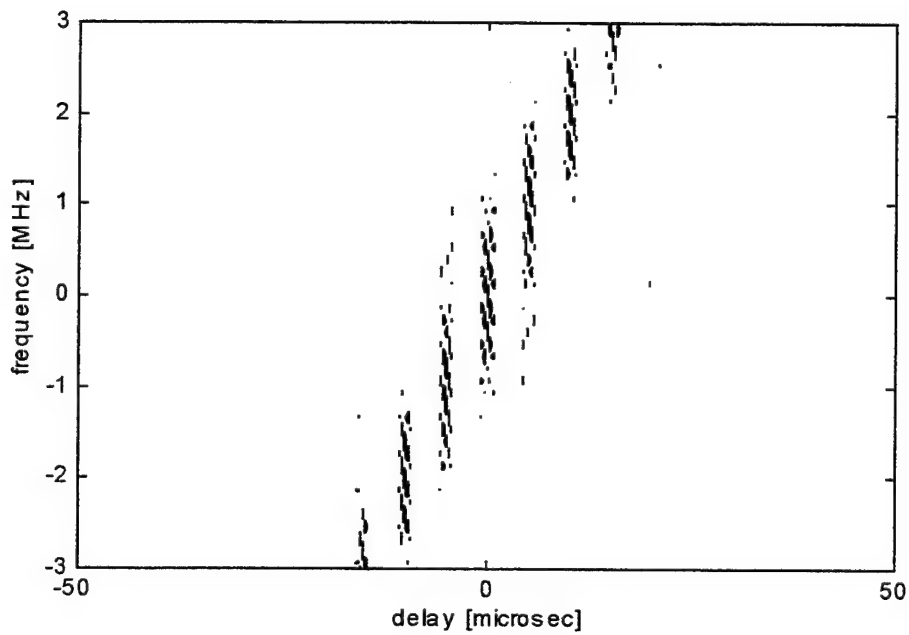(a) Global view.
(b) Magnified view.

domain at f_d=0, which portrays only one peak. This suggests that there is no range ambiguity for the waveform if the target doppler is known. Figure 13(b) is a magnification of Figure 13(a) which gives null-to-null width of 0.4 which is the same as computed from the formula $2/(N\Delta f)$. Note that this is also the output of the matched filter in the time domain. The range resolution of this waveform is 0.2 as given by $1/(N\Delta f)$. Figure 14(a) is a cut of the ambiguity surface along the frequency domain at τ=0. Theory suggests that there should be $(2T/t_s)$-1 peaks in the frequency domain, which is matched by the actual value of 9. Figure 14(b) is a detail of the central peak and should have a null-to-null width of $2/(NT)$ which matches with the actual value of 0.08.

2. Second waveform

For the second case, the waveform has the same parameters as in the previous one except that the number of pulses is increased to 10. This would affect the range resolution ($1/N\Delta f$) and the doppler resolution ($1/NT$) which are now 0.1 and 0.02 respectively. However, some other quantities of interest such as the component contours in the frequency axis stay the same. The results can be observed in Figures 15 through 18. Figure 15(a) gives the global view of the contour plot of the ambiguity diagram for this waveform. Figures 15(b), 16(a) and 16(b) are successively increasing magnifications of the contour plot. Figure 16(b) is a detailed plot of the central peak giving a range resolution and frequency resolution of 0.1 and 0.02, respectively. This can be confirmed in Figures 17(b) and 18(b) which are magnified views of the time and frequency profiles, respectively.
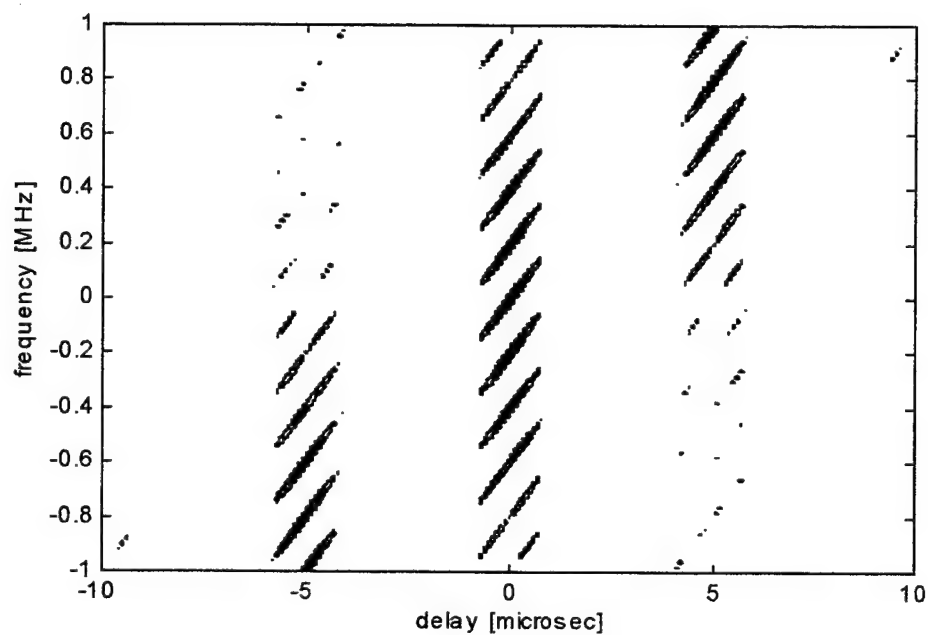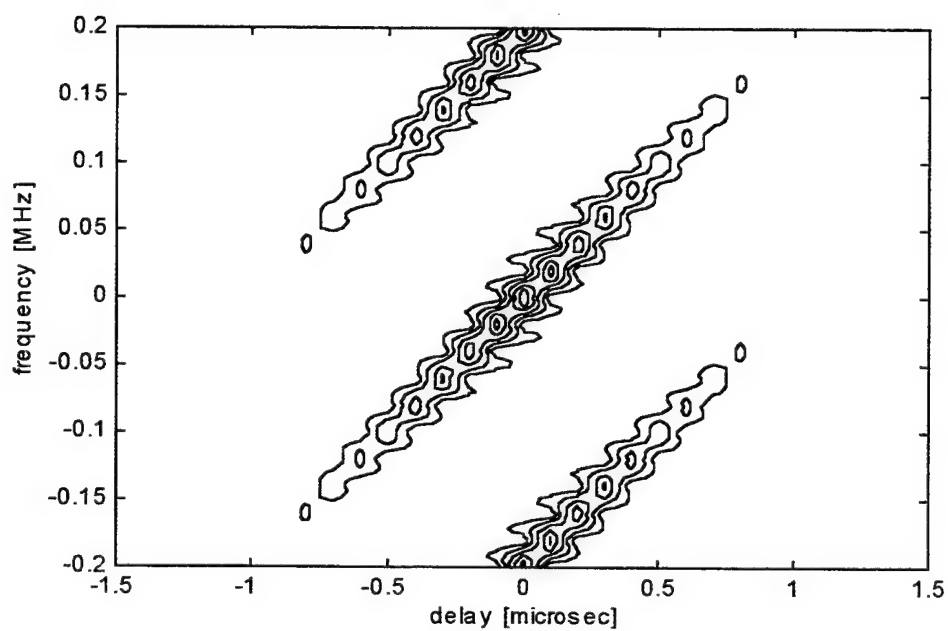
Figure 15. Contour plots of the ambiguity diagram of a step frequency waveform.
(N=10, pulse width=1 microsec, PRI=5 microsec, Δf=1 MHz)
(a) Global view.
(b) Magnified view.

40

Figure 16. Contour plots of the ambiguity diagram of a step frequency waveform.
(N=10, pulse width=1 microsec, PRI=5 microsec, Δf=1 MHz)
(a) Magnified view.
(b) Magnified view of the central peak.

41

Figure 17. Time profiles (cut at zero frequency) of the ambiguity diagram of a step
frequency waveform. (N=10, pulse width=1 microsec, PRI=5 microsec,
Δf=1MHz)

(a) Global view.
(b) Magnified view.

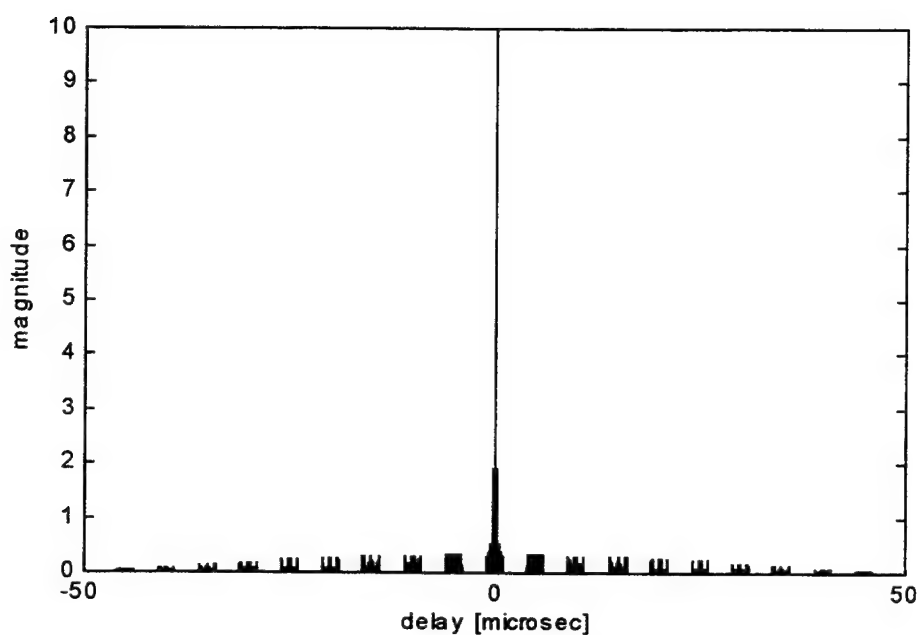Figure 18. Frequency profiles of the ambiguity diagram of a step frequency waveform. (N=10, pulse width =1 microsec, PRI=5 microsec, Δf=1MHz)
(a) Global view.
(b) Magnified view.

3. Third waveform

For this waveform the pulse width is reduced to 0.1 μs and the rest of the parameters are the same as in the previous case. The results can be observed in Figures 19 through 24. Figure 21 represents the central peak of the ambiguity diagram of this step frequency waveform which is similar to the one in Figure A.7.

Now that all the theoretical dimensions previously defined were verified, they can be used to calculate the dimensions of any particular case of interest. This will be done for the fourth and last case.
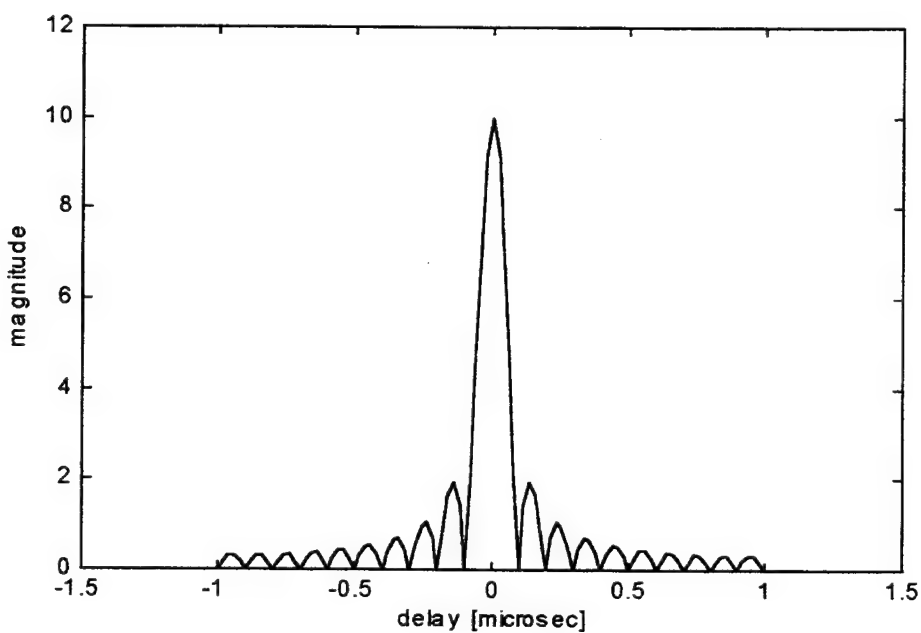
Figure 19. Contour plot of the ambiguity diagram of a step frequency waveform.
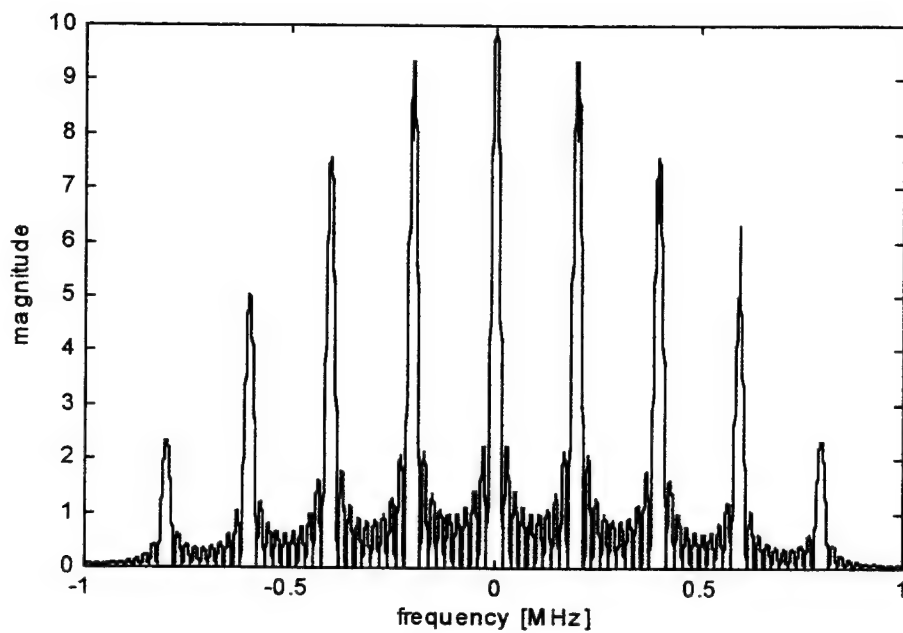(N=10, pulse width=0.1 microsec, PRI=5 microsec, Δf=1 MHz)

Figure 20. Time profile (cut at zero frequency) of the ambiguity diagram of a step
frequency waveform. (N=10, pulse width=0.1 microsec, PRI=5 microsec
Δf=1 MHz)

45

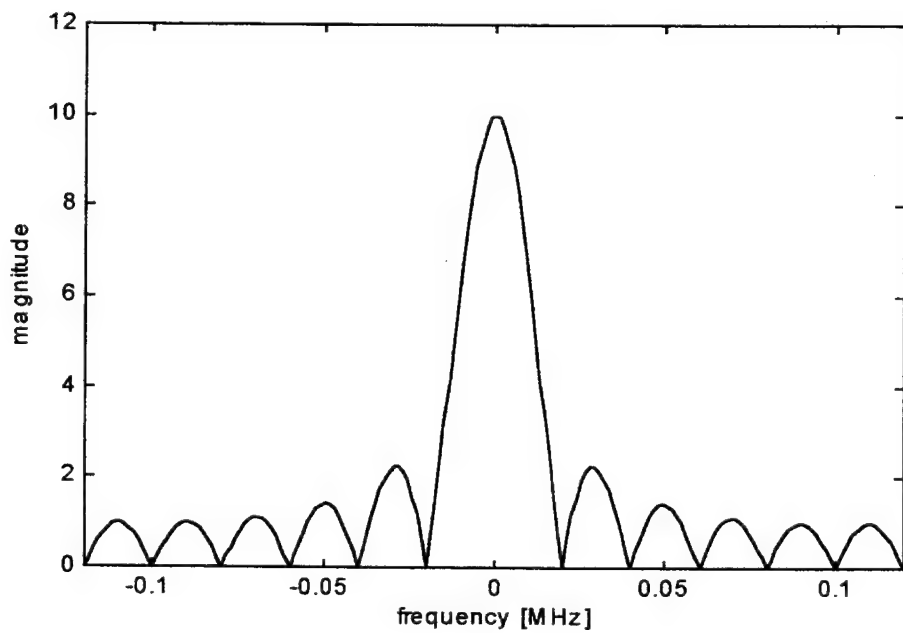Figure 21. 3D plot of the central peak of the ambiguity diagram of a step frequency
waveform. (N=10, pulse width=0.1 microsec, PRI=5 microsec,Δf=1 MHz)

Figure 22. Contour plot of the central peak of the ambiguity diagram of a step
frequency waveform. (N=10, pulse width=0.1 microsec, PRI=5 microsec,
Δf=1 MHz)

46

Figure 23. Time profile (cut at zero delay) of the central peak of the step frequency waveform. (N=10, pulse width = 0.1 microsec, PRI = 5 microsec, Δf=1MHz)

Figure 24. Frequency profile (cut at zero delay) of the central peak of a step frequency waveform. (N=10, pulse width=0.1 microsec, PRI=5 microsec, Δf=1 MHz)

47

4.   Fourth waveform

Using the results from Section B, which have been confirmed for the waveforms discussed so far, ambiguity diagram figures were sketched for a waveform with 500 pulses. The amount of computations required to generate the ambiguity surface by computer is enormous. The 3D ambiguity diagram of this waveform is several magnitudes more complex than 3D pictures of midtown Manhattan. One can realize the problem of resolution of this figure and its printing on a normal size paper or even in a much larger size one.

A contour plot of the ambiguity diagram is sketched in Figure 25. Each short slant line is a spike. In doppler dimension the spikes are PRF (200 KHz) apart and spread over $2/t_s$ (20 MHZ). In delay dimension (at $f_d=0$) there are about ten significant spikes (in reality there are more but others will be small in magnitude). This means that the IF filter will pass ten frequency lines, which implies that the return from ten different ranges due to separate pulses may arrive at the same time. Thus, one may say that the target will be ambiguous in range and that it can lie in any of the ten range zones. Apart from the fact that the target range ambiguity needs to be resolved it will also compete against clutter from ten different range zones.

If the waveform PRF is high, the doppler from a target moving at the highest expected velocity may be kept unambiguous. In such cases, spikes along the doppler dimension may be ignored, otherwise they have to be considered for clutter calculations. Figures 26 and 27 represent cuts along the delay and frequency dimensions indicating the potential range and doppler ambiguities, respectively. Figure 28 gives the detail of the central peak (note that other peaks or spikes are of similar shape but may be of different magnitude and located at

48

different places in range-doppler map). At f_d=0 the peak is 4 ns wide (null-to-null) in delay dimension. Similarly, the width of the peak in frequency dimension (at τ=0) is given by 2/NT which comes out to be 800 Hz.
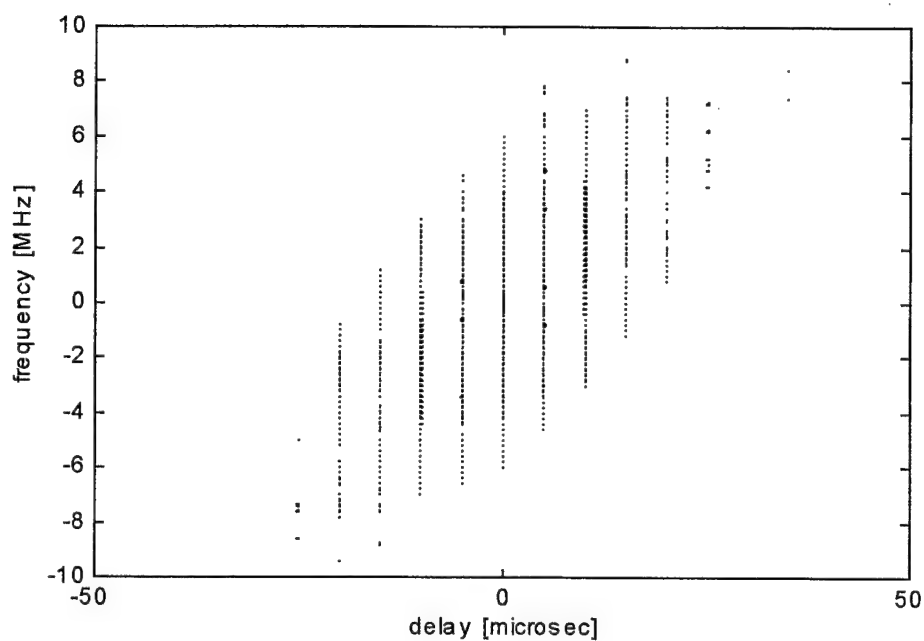
Figure 25. Contour plot of the ambiguity diagram of a step frequency waveform.
(N=500, pulse width=0.1 microsec, PRI=5 microsec, Δf=1 MHz)

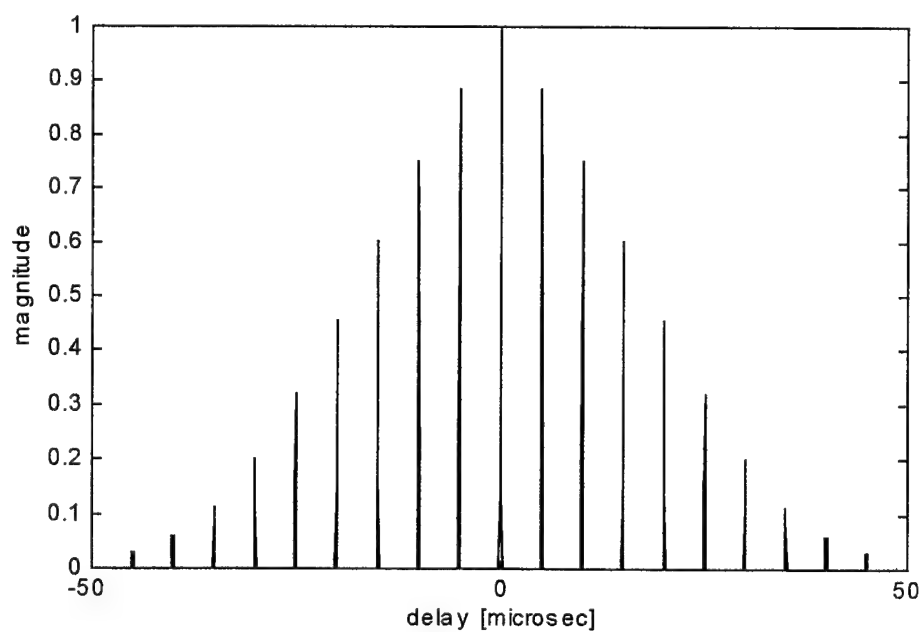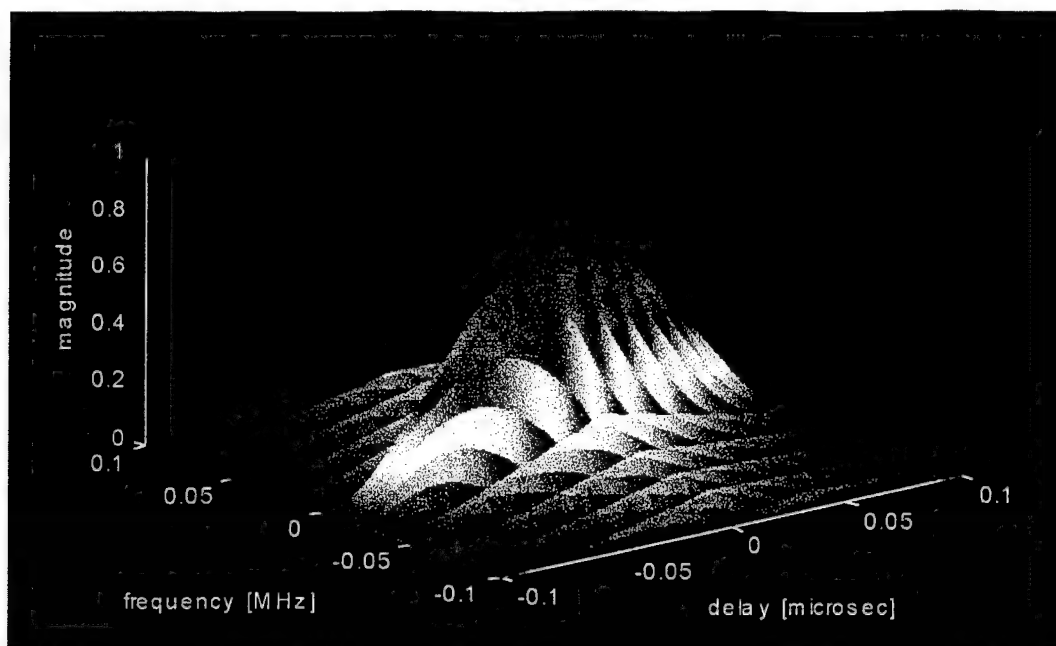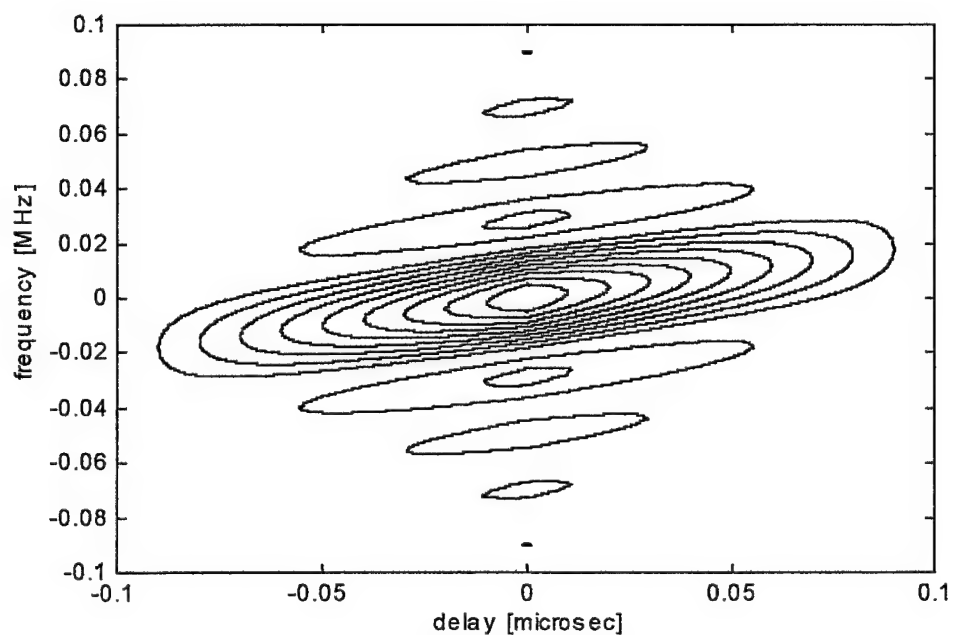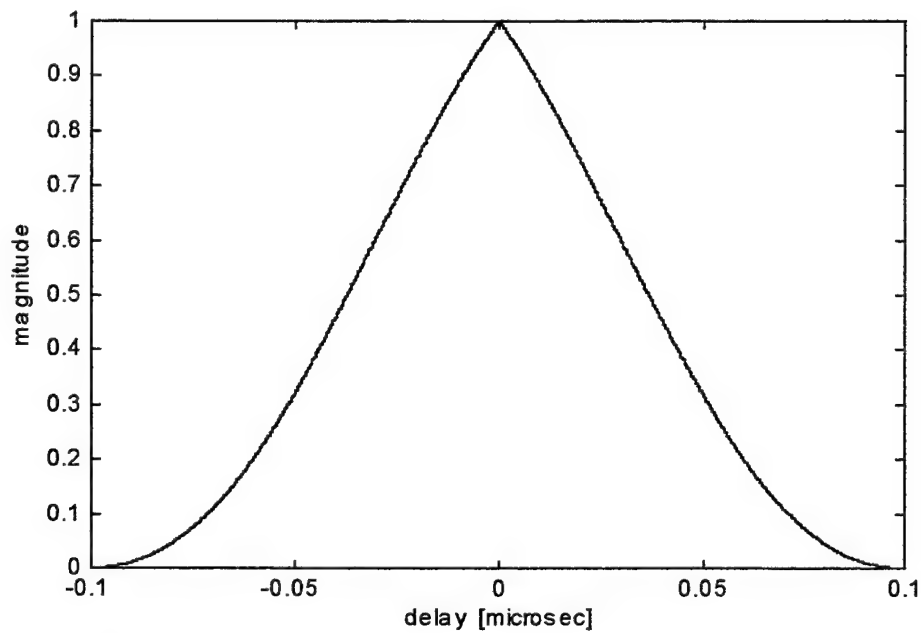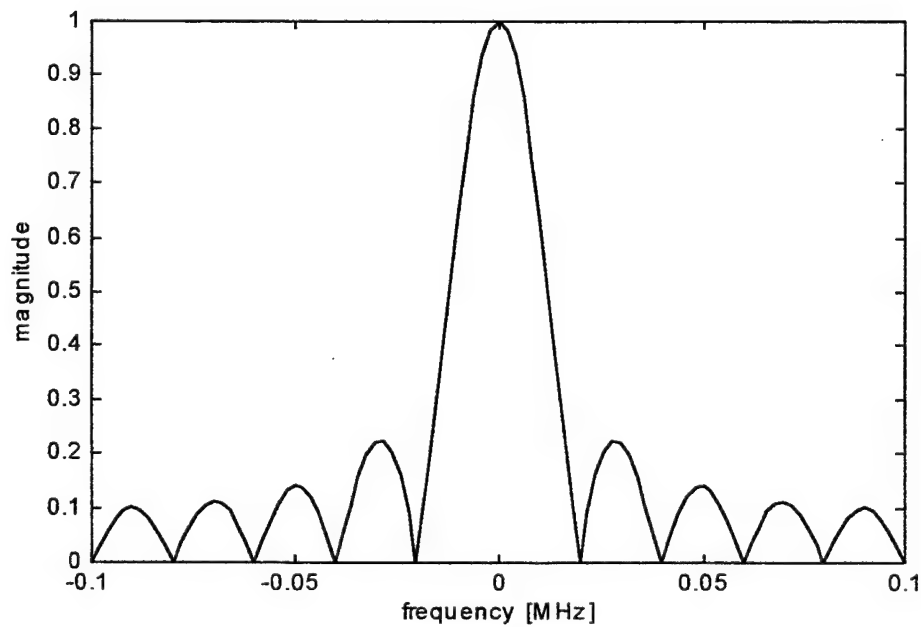Figure 26. Time profile (cut at zero frequency) of the ambiguity diagram of a step frequency waveform. (N=500, pulse width=0.1 microsec, PRI=5 microsec, Δf=1 MHz)

51

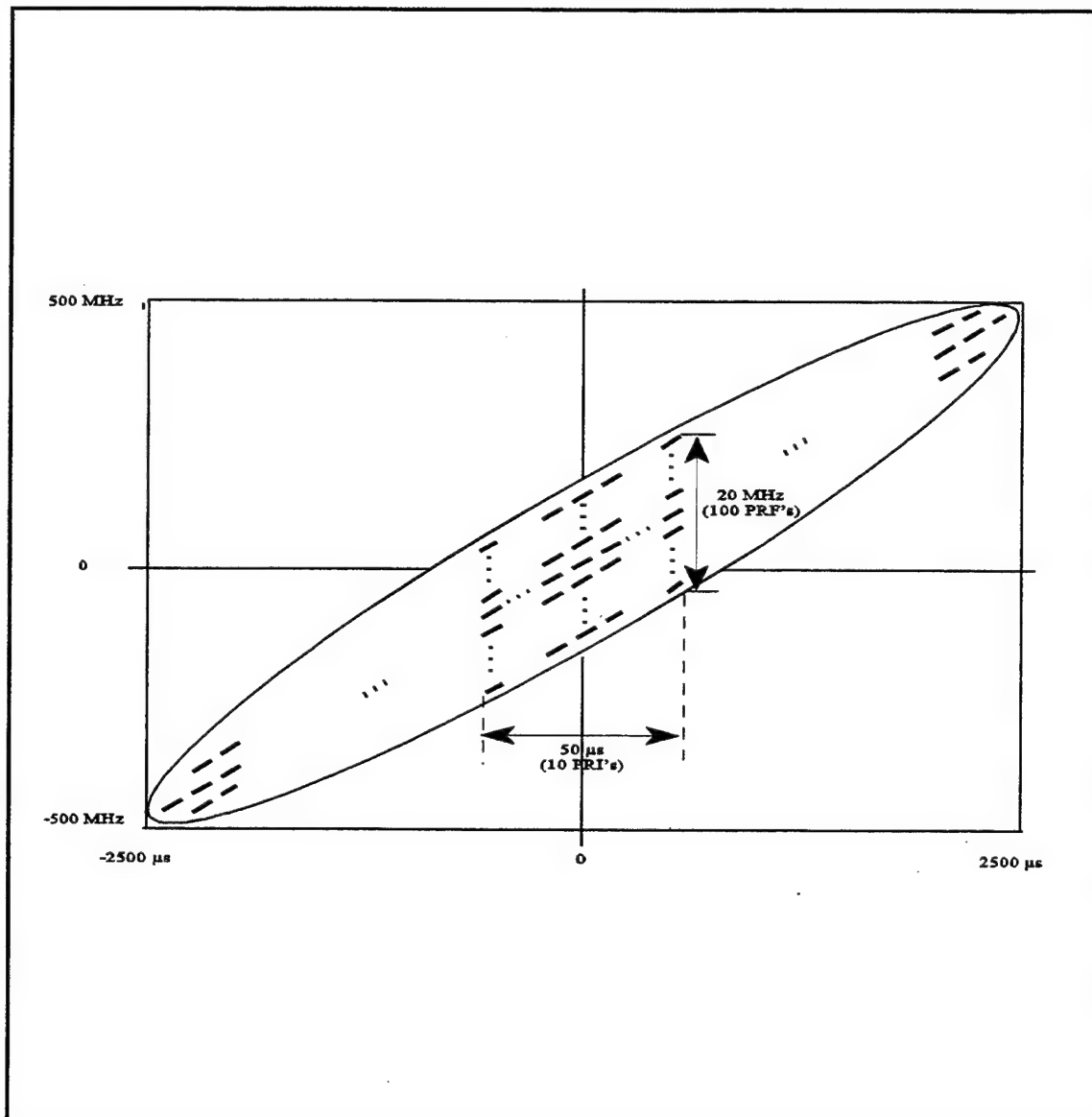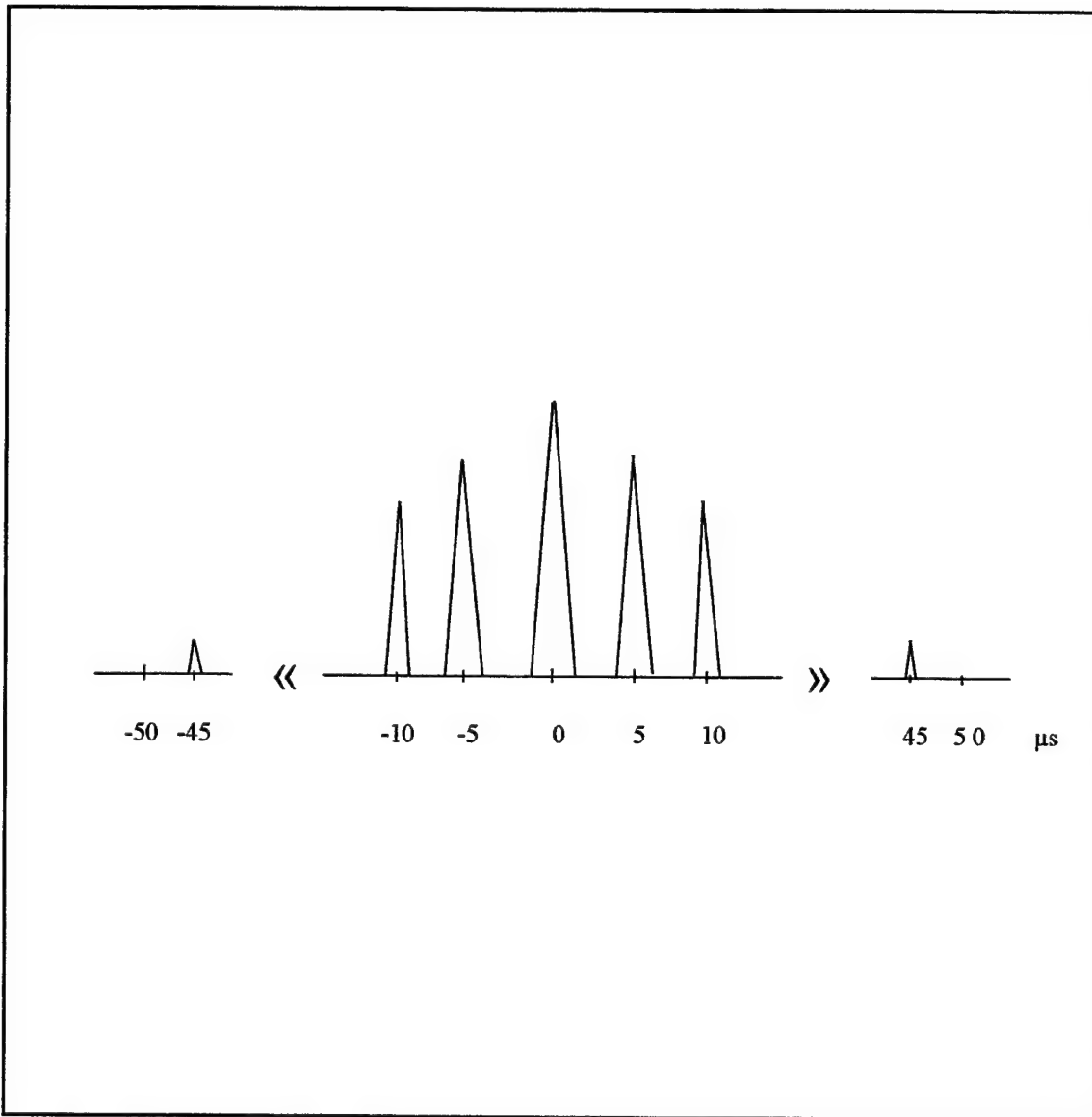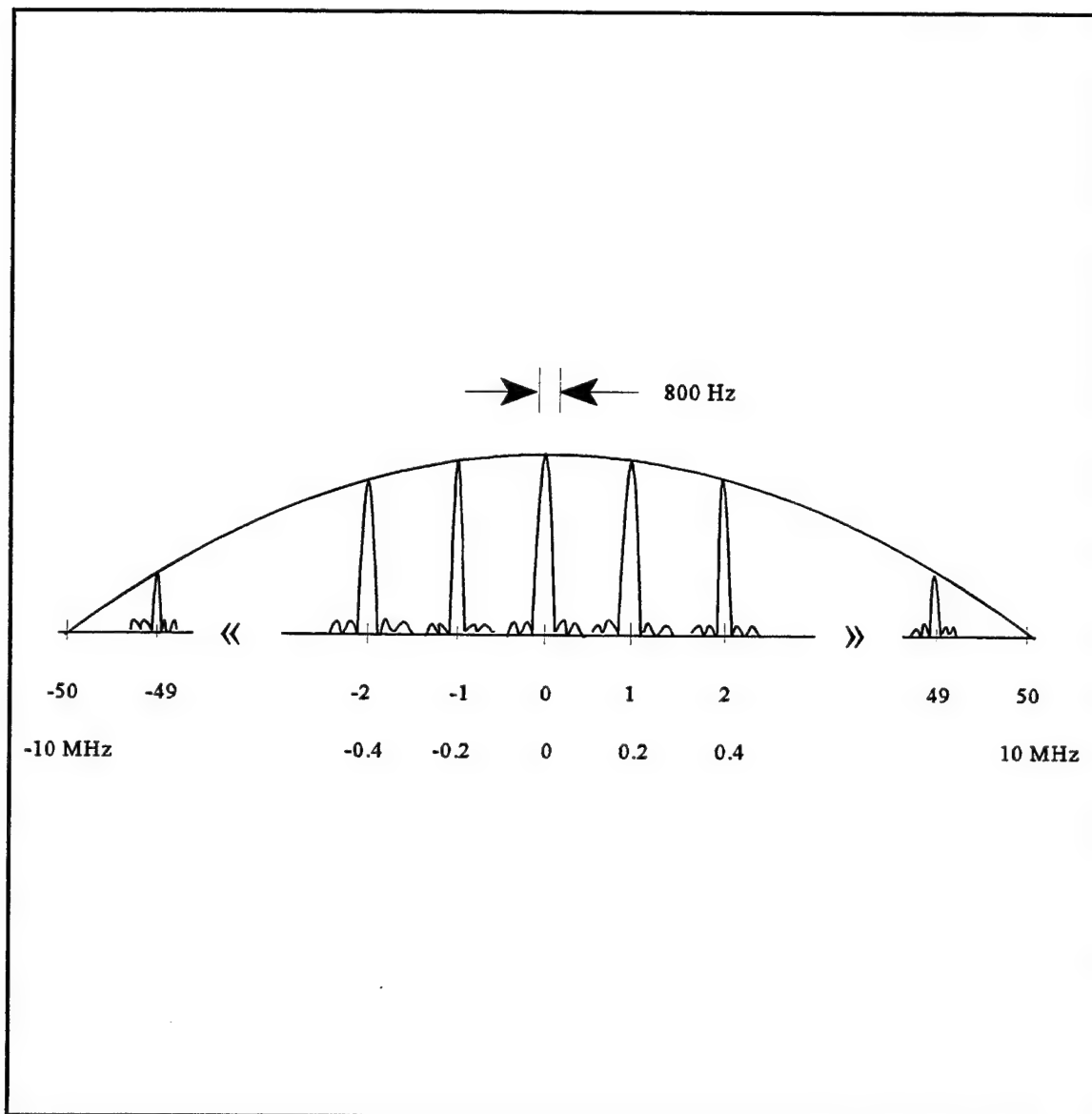Figure 27. Frequency profile (cut at zero delay) of the ambiguity diagram of a step frequency waveform. (N=500, pulse width=0.1 microsec, PRI=5 microsec, Δf=1 MHz)
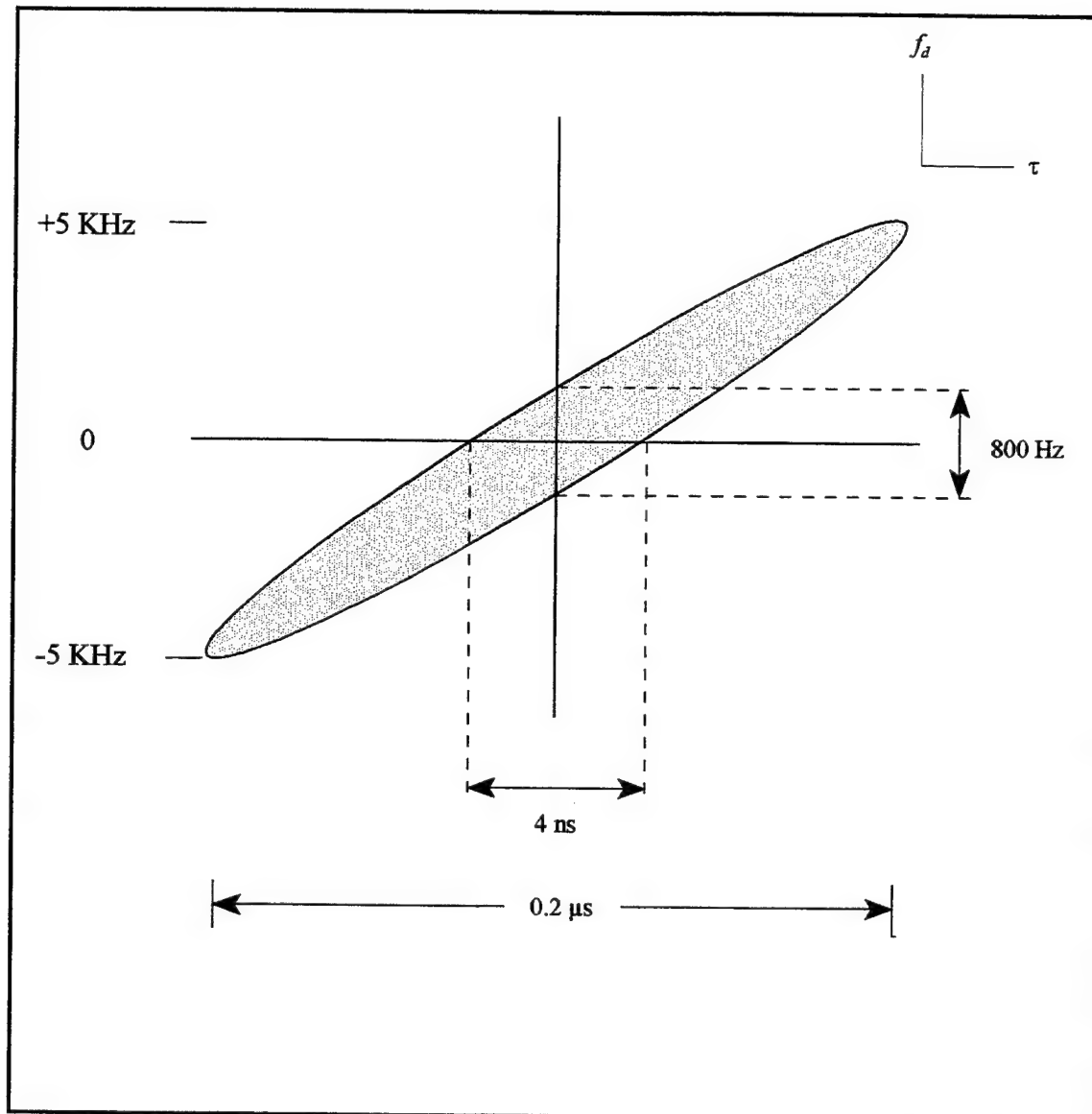
Figure 28. Dimensions of the central peak for the case N=500, pulse width = 0.1 µs, PRI = 5 µs, Δf = 1 MHz. (Values indicated are null-to-null; generally 3dB values are given which are a little less than half of the indicated.)

V. CONCLUSIONS

Step frequency has several unique features and advantages over conventional high resolution waveforms. It simultaneously allows pulse compression and doppler processing. It can be implemented on existing radars with the addition of a frequency synthesizer and suitable signal processing. This waveform achieves high resolution with narrow instantaneous bandwidth and thus reduces the requirements on A/D sampling rate. Further, more multiple time around clutter is kept limited by judicious choice of waveform parameters which reduces the amount of clutter entering the IF amplifier. This in turn reduces the requirement for dynamic range of A/D. It is difficult to achieve high sampling rate in A/D when combined with large dynamic range. Lowering the requirement on sampling rate and dynamic range makes the implementation of high resolution systems feasible.

In this report, emphasis is put on the design of a waveform for surface based radars to detect small moving targets. Because of the many tradeoffs involved in the design of a step frequency waveform, the choice of the waveform parameters is not straight forward. To systematize the waveform parameter choice, a design procedure was developed for step frequency waveform. The proposed method determines the waveform parameters for given radar specifications. Two different implementations of this method were presented: the graphical and the computer implementation. The graphical implementation is a simple and quick way of calculating the minimum design parameters. The computer implementation takes into account parameter constraints imposed by the hardware.

The ambiguity diagram for a specific waveform of interest to NaRD was developed. Since the waveform consists of a large number of pulses it is almost impossible to directly

54

compute the ambiguity function. Therefore, waveforms with parameter close to the waveform of practical interest but easier to compute were investigated, in order to bring out the key characteristics of the waveform of interest. The theoretical dimensions of the step frequency waveform were defined and verified with a few cases. Once this was done, the particular case of interest was investigated. It contains the elements of ambiguity function of a single LFM pulse and a train of constant frequency pulses. The 3D plot of the ambiguity function of a step frequency waveform is spiky like the one of a constant frequency pulse train and is tilted at an angle like the ambiguity diagram of a LFM pulse. The width of the central spike along the delay axis at zero frequency is $2/(N\Delta f)$ as compared to $2t_s$ for the constant frequency pulse train, thus verifying the high range resolution potential of this waveforms. The range resolution can be increased by increasing the product $N\Delta f$ (and without decreasing the pulse width). For the constant frequency pulse train, high range resolution can only be improved by decreasing the pulse width. On the frequency axis, the spike width at zero delay is equal to $2/(NT)$ as also is the case for the constant frequency pulse train. Therefore, the frequency resolution for the step frequency waveform is the same as for the constant frequency waveform.

Further work on the comparative analysis of step frequency waveform should be performed to compare it with conventional high PRF and medium PRF waveforms for detection of small targets. Its use in inverse synthetic aperture radar (ISAR) for moving target identification should also be investigated.

55

APPENDIX A

A. DEFINITION OF AMBIGUITY FUNCTION AND ITS PROPERTIES

1. Definition of Ambiguity Function

A radar waveform's ambiguity function is probably the most complete statement of the waveform's inherent performance. It is a formula that quantitatively describes the interference caused by a point target return located at a different range and velocity from a reference target of interest. It reveals the range-doppler position of ambiguous responses and defines the range and doppler resolution. [Ref. 2, pp. 74]

This quantitative description of the ability of a waveform to resolve two or more radar reflectors at arbitrarily different ranges and velocities, constitutes an important feature for quick assessment of the interference level with which a target of interest must compete when it is in the vicinity of other radar reflectors. Although it is seldom used as a basis for practical radar system design, it provides an indication of the limitations and utility of particular classes of radar waveforms, and gives the radar designer general guidelines for the selection of suitable waveforms for various applications.

The ambiguity function of the waveform $s(t)$ can be defined in terms of the cross-correlation of a doppler-shifted version of the waveform, that is $s(t)\exp(j2\pi f_d t)$ with the unshifted waveform. Using the definition of cross-correlation, it follows that

$$\chi(\tau, f_d) = \int_{-\infty}^{+\infty} \left[s(t) e^{j2\pi f_d t} \right] \left[s^*(t-\tau) \right] dt ,$$

(A.1)

where τ is the delay time and f_d is the doppler frequency shift. Rearranging the terms in the

integral produces a common form of the ambiguity function as shown in Equation A.2.

$$|\chi(\tau, f_d)| = \left| \int_{-\infty}^{+\infty} s(t)\, s^*(t-\tau)\, e^{j2\pi f_d t}\, dt \right| .$$

(A.2)

A normalized expression is obtained by requiring that

$$\int_{-\infty}^{+\infty} |s(t)|^2 dt = 1 .$$

(A.3)

With this normalization, the magnitude of the ambiguity function has a value of unity at the origin.

2.   Properties of the Ambiguity Function

The ambiguity function has the following properties:

$$\text{Peak value of } |\chi(\tau, f_d)| = |\chi(0,0)| = E ,$$

(A.4)

$$|\chi(-\tau, -f_d)| = |\chi(\tau, f_d)| ,$$

(A.5)

$$|\chi(\tau, 0)| = \left| \int_{-\infty}^{+\infty} s(t)\, s^*(t-\tau)\, dt \right| ,$$

(A.6)

$$|\chi(0, f_d)| = \left| \int_{-\infty}^{+\infty} s^2(t)\, e^{j2\pi f_d t}\, dt \right| ,$$

(A.7)

$$\int_{-\infty}^{+\infty} \int_{-\infty}^{+\infty} |\chi(\tau, f_d)|\, d\tau\, df_d = E .$$

(A.8)

Equation A.4, states that the peak value of the ambiguity function occurs at the origin and it

58

is equal to E, the energy contained in the echo signal. Equation A.5 shows the ambiguity function's symmetry. Equation A.6 indicates that the ambiguity function along the time delay axis is the auto-correlation function of the complex envelope of the transmitted signal. Equation A.7 states that along the frequency shift axis the ambiguity function is proportional to the spectrum of s^2 (t). Finally, Equation A.8 states that the total volume under the ambiguity surface is a constant equal to E.

3.   Ambiguity Diagram

It is common to refer to $|\chi(\tau, f_d)|$ as the ambiguity surface of the waveform. The shape of this ambiguity surface depends entirely on the waveform parameters. The plot of the ambiguity surface is called *ambiguity diagram*. The ideal ambiguity diagram consists of a single spike of infinitesimal thickness at the origin and is zero everywhere else. The single center spike eliminates any ambiguities, and its infinitesimal thickness at the origin permits the frequency and the echo delay time to be determined simultaneously to an high degree of accuracy. It also permits the resolution of two targets no matter how close together they are on the ambiguity diagram. Naturally, this ideal diagram does not exist. The two reasons for this can be found in the properties: first, and accordingly with Equation A.4, the maximum height of the ambiguity function is E and secondly the volume under the surface must be finite and equal to E, as stated by Equation A.8. However, a reasonable approximation is given in Figure A.1. This ambiguity function only has one peak and therefore does not cause any ambiguity. However the single peak might not be narrow enough to satisfy the requirements of accuracy and resolution. If the single central peak is made too narrow, it may cause other smaller peaks to occur in regions other than the origin, and therefore cause ambiguities. The
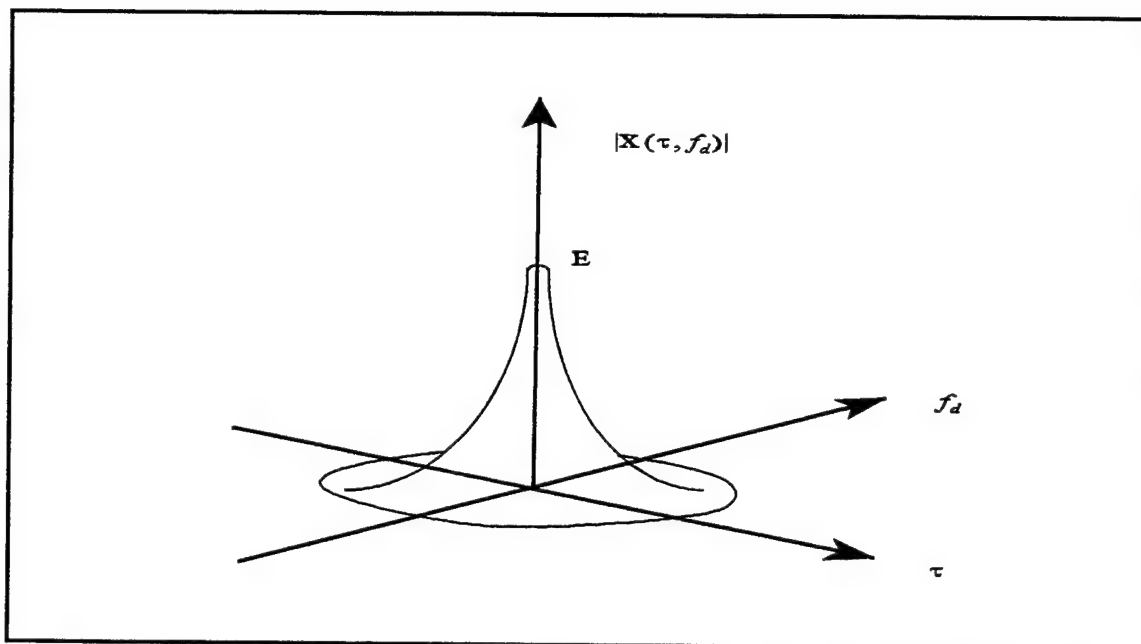
Figure A.1. An approximation to the ideal ambiguity diagram "After Ref. [1]."

requirements for accuracy and unambiguity are not always possible to satisfy simultaneously.

The particular waveform transmitted by a radar is chosen to satisfy the requirements for (1) detection, (2) measurement accuracy, (3) resolution, (4) ambiguity, and (5) clutter rejection. The ambiguity diagram may be used to assess how well a waveform can achieve these requirements. Each of these will be discussed briefly.

The requirements for *detection* do not place any demands on the shape of the transmitted waveform except that it be possible to achieve with practical radar transmitters, and the maximum value of the ambiguity function is an indication of the detection capabilities of the radar. The *accuracy* with which the range and the velocity can be measured by a particular waveform depends on the width of the central spike along the time and frequency axis. The *resolution* is also related to the width of the central spike, but in order to resolve two closely spaced targets the central spike must be isolated. It cannot have any high peaks nearby that can mask another target close to the desired target. A waveform that yields good

60

resolution will also yield good accuracy, but the reverse is not always so.

A continuous waveform (a single pulse) produces an ambiguity diagram with a single peak. A discontinuous waveform can result in peaks in the ambiguity diagram at other values of τ, f_d. The pulse train is a common example. The presence of additional spikes can lead to *ambiguity* in the measurement of target parameters. An ambiguous measurement is one in which there are several choices available for the correct value of a parameter, but only one choice is appropriate. Thus the correct value is uncertain. The ambiguity diagram permits a visual indication of the ambiguities possible with a particular waveform. The ambiguity problem, detection and accuracy are related to a single target, whereas resolution applies to multiple targets.

The ambiguity diagram may be used to determine the ability of a waveform to reject clutter by superimposing on the τ, f_d plane the regions where clutter is found. If the transmitted waveform is to have good *clutter-rejection* properties the ambiguity function should have little or no response in the regions of clutter.

The problem of synthesizing optimum waveforms based on a desired ambiguity diagram specified by operational requirements is not normally feasible. The approach to selecting a waveform with a suitable ambiguity diagram is not systematic but rather by trial and error.

The name *ambiguity function* is somewhat misleading since this function describes more about the waveform than just its ambiguity properties. This name was given to this function in order to demonstrate that the total volume under it, is a constant equal to E, independent of the shape of the transmitted waveform. Thus the total area of ambiguity, or

uncertainty, is the same no matter how the ambiguity surface is distributed over the τ, f_d plane. [Ref. 1, pp. 418-420]

B. AMBIGUITY FUNCTION OF A SINGLE PULSE

The unmodulated single pulse is widely used in old generation radars for search and track functions (as magnetrons are not easily modulated) and where range accuracy and resolution requirements can be met with a pulse wide enough to provide sufficient energy for detection. It has the minimum ratio of time sidelobe extent to compressed pulse width and is used in inexpensive radars where signal generation and processing costs must be minimized.

The single pulse of a sine wave can be defined as

$$S(t) = s(t)e^{j2\pi f_0 t} , \qquad (A.9)$$

where $s(t)$ is the complex envelope of the signal, defined as follows:

$$s(t) = 1, \quad \text{if } 0 \le t \le t_s,$$
$$= 0, \quad \text{elsewhere}, \qquad (A.10)$$

with t_s equal to the pulse width.

Using Equation A.2, the ambiguity function of the single pulse can be written as follows:

$$|\chi(\tau, f_d)| = |\int_{\tau}^{t_s} e^{j2\pi f_d t} dt|$$

$$= \left| \left(1 - \frac{|\tau|}{t_s}\right) \frac{\sin[\pi t_s (1 - |\tau|/t_s) f_d]}{\pi t_s (1 - |\tau|/t_s) f_d} \right| , \quad \text{if } |\tau| \le t_s ,$$

zero elsewhere. $\qquad$ (A.11)

62

The ambiguity diagram of the single pulse is shown in Figure A.2 and the contour plot can be observed in Figure A.3. Profiles of the ambiguity function, taken through its peak, are shown in Figures A.4 and A.5. The time profile is a triangle (the autocorrelation of a rectangle is a triangle) with a half-voltage width equal to the pulse width. The frequency profile is a sinc function whose main lobe width is twice the reciprocal of the pulse width.
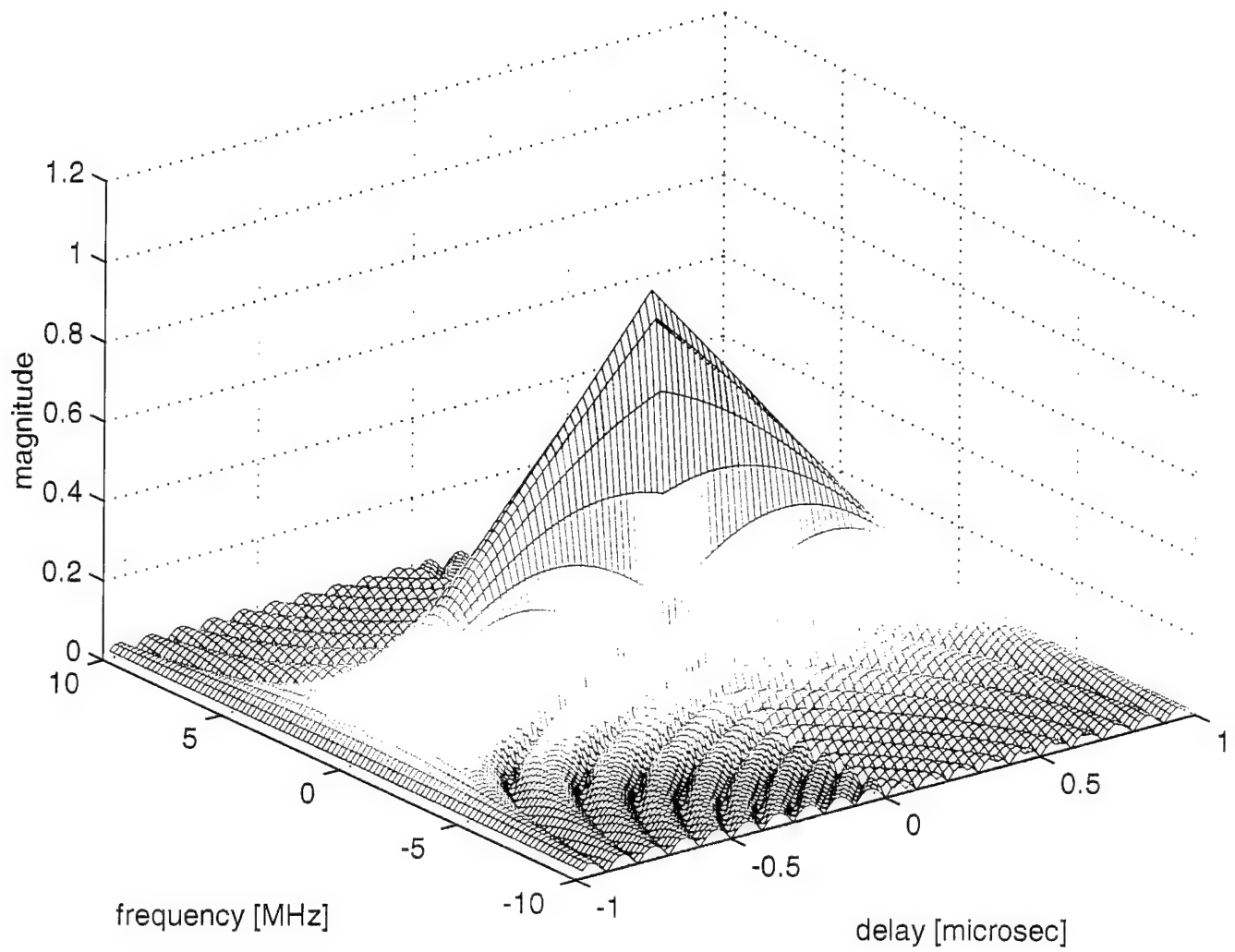
Figure A.2.   Ambiguity diagram of a single pulse.
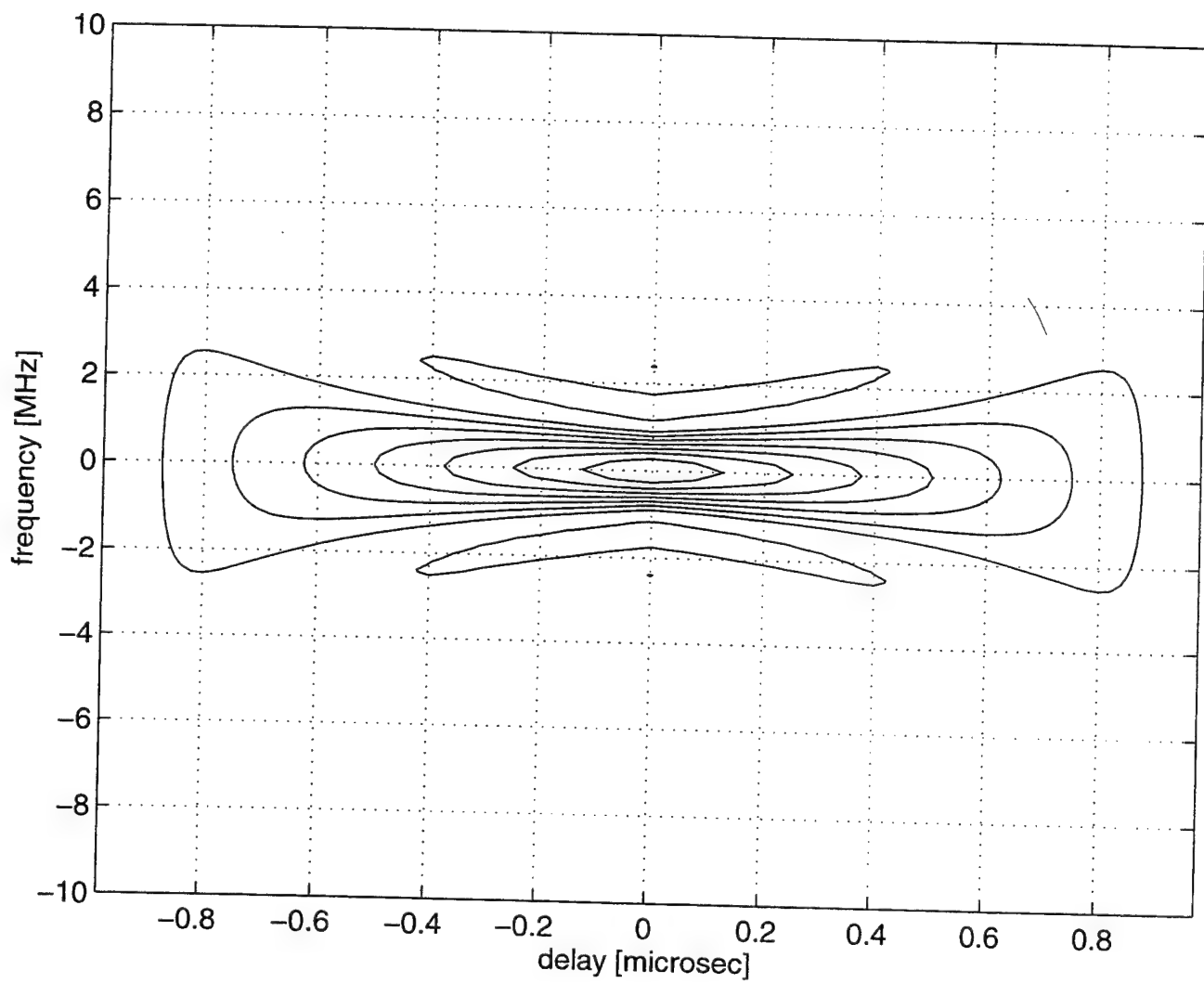(pulse width=1 microsec)

64

Figure A.3. Contour plot of the ambiguity diagram of a single pulse.
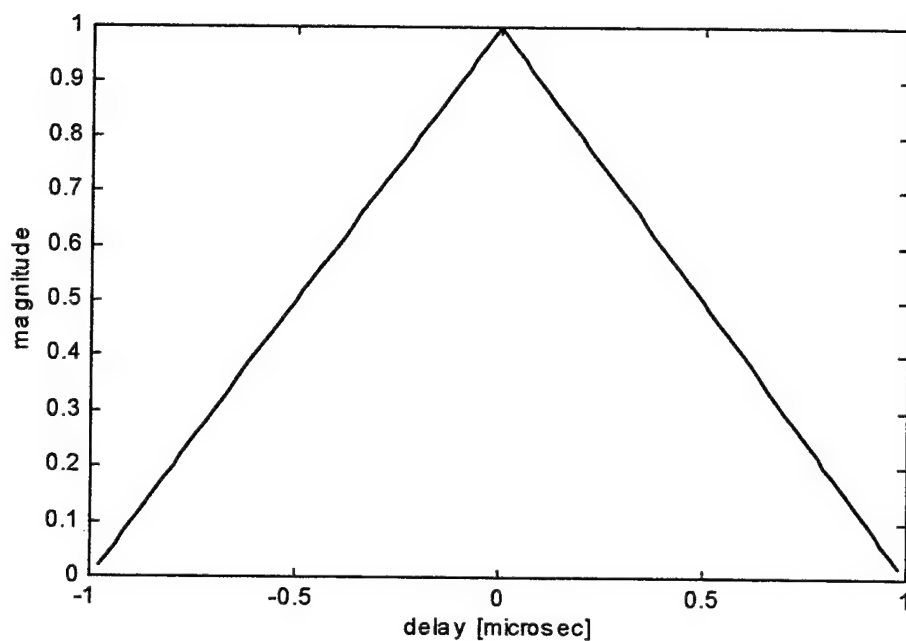
(pulse width=1 microsec)

Figure A.4 Time profile of the ambiguity diagram of a single pulse.
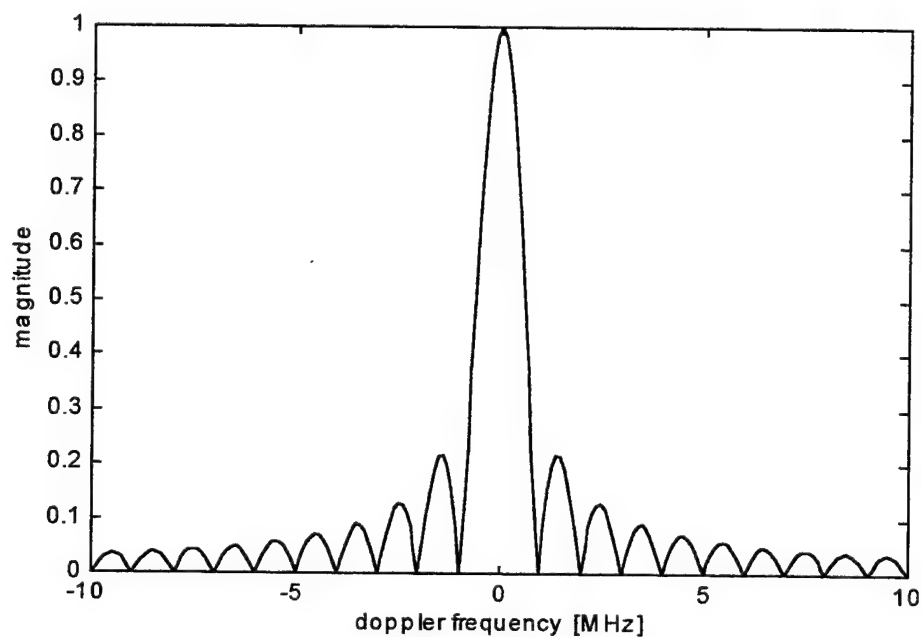(pulse width =1 microsec)

Figure A.5. Frequency profile of the ambiguity diagram of a single pulse.
(pulse width =1 microsec)

C. AMBIGUITY FUNCTION OF THE LINEAR FREQUENCY MODULATED PULSE

The linear frequency modulated (LFM) pulse is commonly used to increase range accuracy and resolution when long pulses are required to get reasonable signal-to-noise ratios (10 to 20 dB). This waveform can be used for detection of targets with unknown velocity since the doppler sensitivity is low.

The LFM pulse can be represented mathematically as

$$
\begin{aligned}
S(t) &= s(t)\, e^{j2\pi\left(f_0 t + \frac{1}{2}k t^2\right)} \\
&= \left[s(t)\, e^{j\pi k t^2}\right] e^{j2\pi f_0 t} ,
\end{aligned}
\tag{A.12}
$$

where $s(t)$ is the same as defined in Equation A.10, and k is the rate of frequency change in Hz/sec. The ambiguity function of the LFM pulse can be written as in Equation A.13.

$$
\begin{aligned}
|\chi(\tau, f_d)| &= \left| \int_{-\infty}^{+\infty} s(t)\, s^*(t-\tau)\, e^{j2\pi(f_d - k\tau)t}\, dt \right| \\
&= \left| \left(1 - \frac{|\tau|}{t_s}\right) \frac{\sin[\pi t_s (1-|\tau|/t_s)(f_d + k\tau)]}{\pi t_s (1-|\tau|/t_s)(f_d + k\tau)} \right| , \quad if\ |\tau| \le t_s,
\end{aligned}
$$

$$
\text{zero elsewhere.} \tag{A.13}
$$

Comparing this equation with Equation A.2, we can see that they are identical, except that f_d is replaced by $f_d - k\tau$. Therefore, we can conclude that the ambiguity function of the LFM pulse is a shifted version of the ambiguity function of a single pulse. This relation is represented graphically in Figure A.6 and it can be seen that the ambiguity function of the LFM pulse is just a rotated version of the ambiguity function of the single pulse.
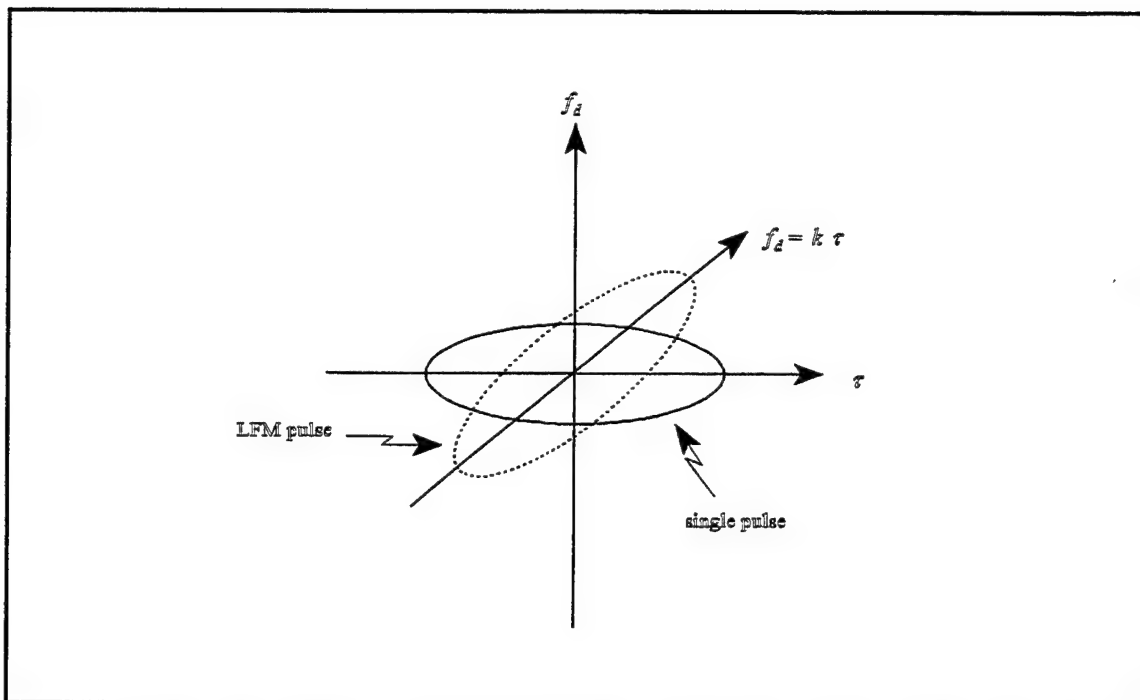
Figure A.6. Contour comparison for the single pulse and the LFM pulse.

Figures A.7, A.8, A.9, and A.10, represent the ambiguity diagram, contour plot, and time and frequency profiles (taken through the peak), respectively.
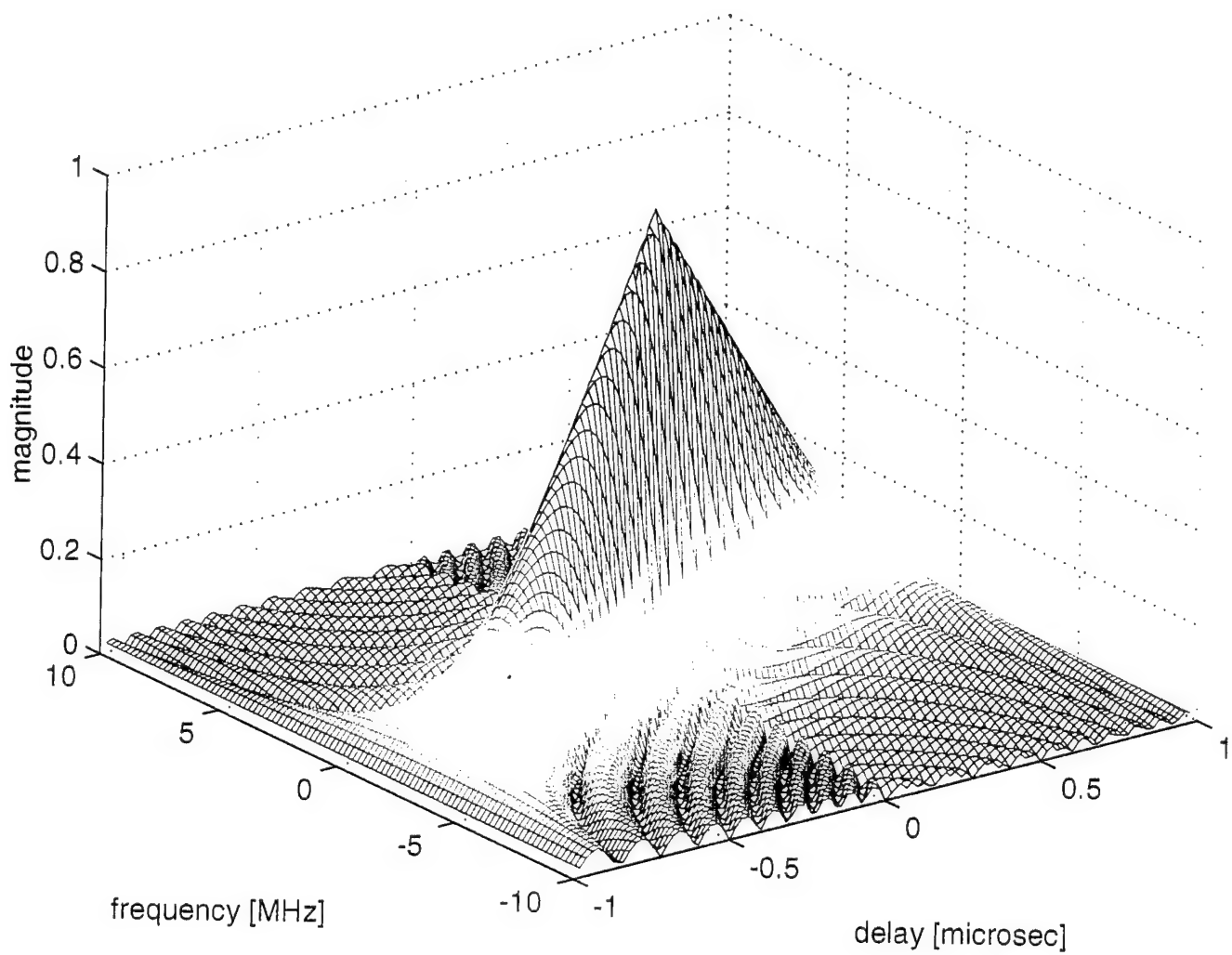
Figure A.7.   Ambiguity diagram of a LFM pulse.

(pulse width=1 microsec)

69
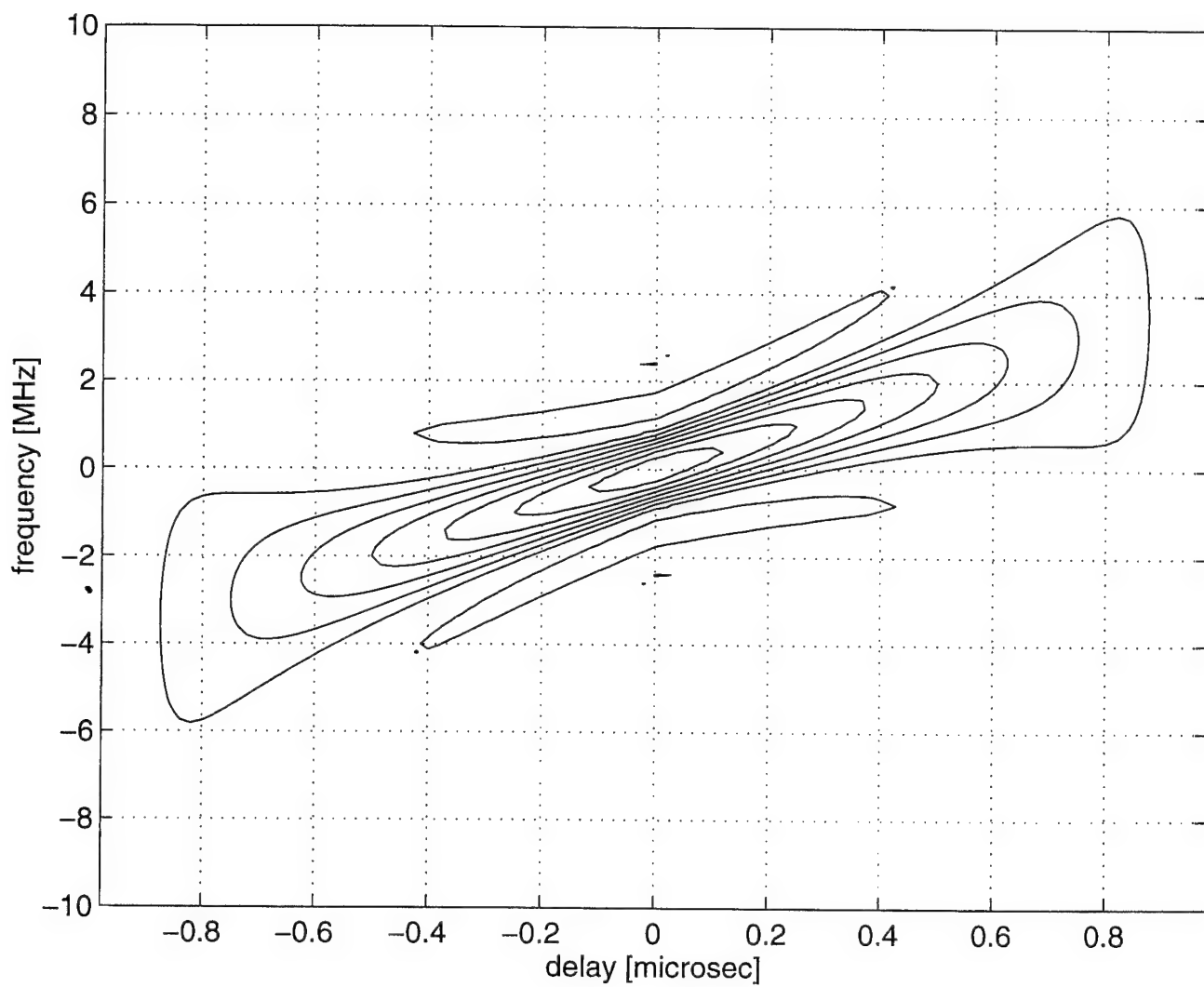
Figure A.8. Contour plot of the ambiguity diagram of a LFM pulse.

(pulse width=1 microsec)
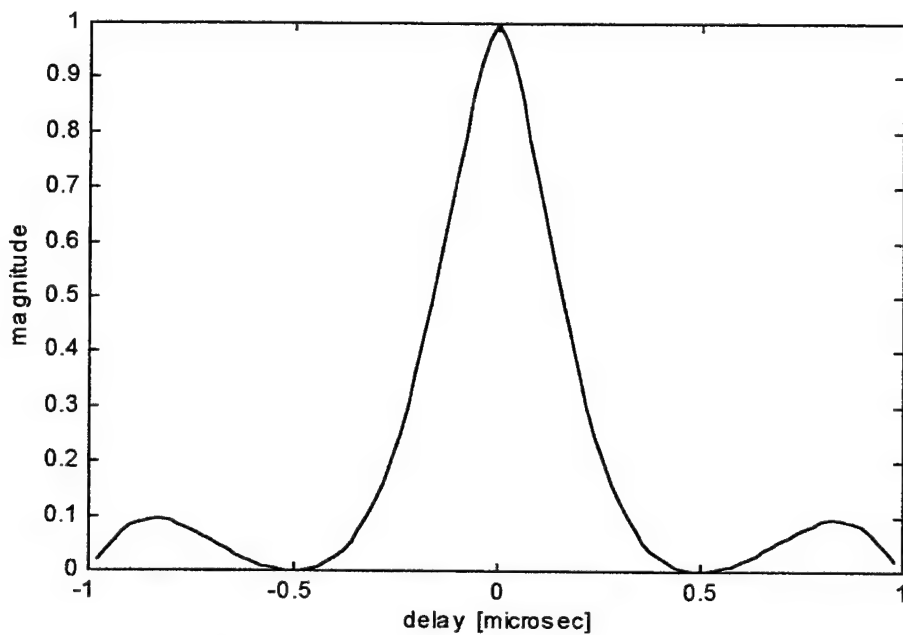
Figure A.9. Time profile of the ambiguity diagram of a LFM pulse.
(pulse width =1 microsec)
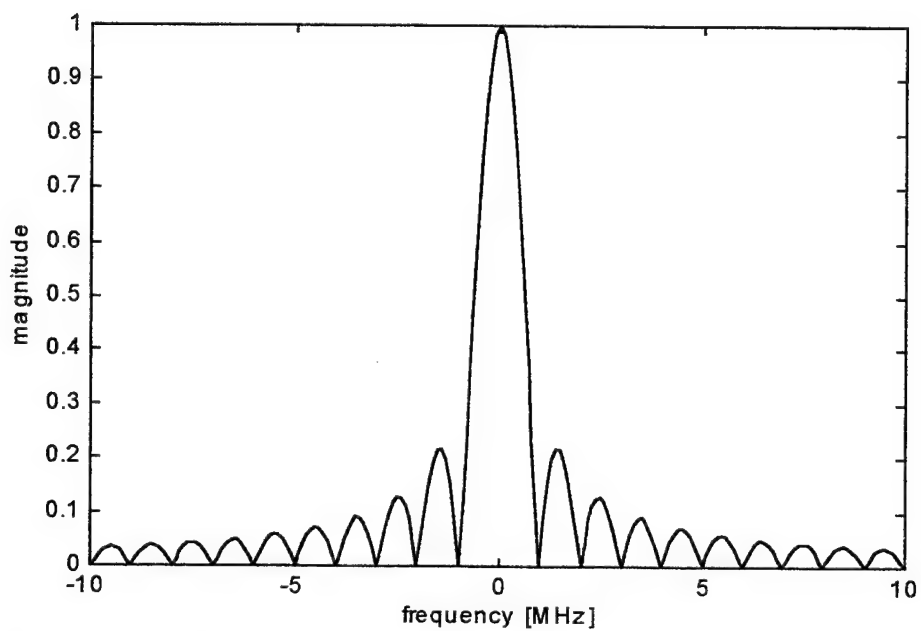
Figure A.10. Frequency profile of the ambiguity diagram of a LFM pulse.
(pulse width =1 microsec)

D. AMBIGUITY FUNCTION OF THE CONSTANT FREQUENCY PULSE TRAIN

Practical radars employ waveforms consisting of constant frequency pulse trains and therefore it is important to study their ambiguity functions. The ambiguity functions for these pulse trains reveal ambiguous responses in range and doppler. Performance for specific surveillance applications can be understood in terms of unambiguous range-doppler regions of operation determined by radar pulse repetition frequency, pulse duration, and pulse bandwidth. For high resolution applications, the ambiguity surface of individual pulses of the pulse train is also of interest. [Ref. 2, pp. 74-75]

For single pulse delay and frequency measurement accuracies depend on the single parameter of pulse width. With the pulse train this situation can be avoided. The delay accuracy depends on the pulse width as before, but the frequency accuracy is now determined by the total duration of the pulse train. Therefore, both accuracies are independent of one another. The price that has to be paid for this capacity of independently controlling delay and frequency accuracies is that additional peaks occur in the diagram, which in turn cause range and doppler ambiguities. In practice, the radar designer tries to select the PRI in order to make all targets of interest appear in the vicinity of the central peak, and all the other peaks occur as far from this region as possible.

Most radars use this type of waveform, which can be mathematically represented as follows:

$$S(t) = \sum_{n=0}^{N-1} s(t-nT) \, e^{j2\pi f_0 t} , \qquad\qquad (A.14)$$

where $s(t)$ is the complex envelope of the single pulse of the transmitted signal, defined as

$$s(t-nT) = 1, \qquad \text{if } nT \le t \le nT+t_s,$$
$$\qquad\qquad = 0, \qquad \text{elsewhere.} \qquad (A.15)$$

In this equation, N is the number of pulses, T is the PRI and t_s is the pulse width. The ambiguity function of the constant frequency pulse train can be written as

$$|\chi(\tau, f_d)| = |\int_{-\infty}^{+\infty} \sum_{n=0}^{N-1} s(t-nT) \sum_{m=0}^{N-1} s^*(t-mT-\tau) e^{j2\pi f_d t} dt|. \qquad (A.16)$$

Changing variables ($t-nT=t'$), Equation A.16 becomes

$$|\chi(\tau, f_d)| = |\sum_{n=0}^{N-1} \sum_{m=0}^{N-1} e^{j2\pi f_d nT} \int_{-\infty}^{+\infty} s(t') \, s^*(t'-(m-n)T-\tau) \, e^{j2\pi f_d t'} dt'|. \qquad (A.17)$$

Figure A.11 is a level contour of the ambiguity surface of a constant frequency pulse train. This figure shows that the width of the central peak along the delay axis is approximately twice the pulse width, and that along the frequency axis is 2/NT. The interpeak distance along the delay axis is equal to the PRI, and along the frequency axis 1/PRI, which is the PRF of the waveform. The total non-zero extent along the delay axis is 2NT and along the frequency axis is 2/t_s. Figure A.12 represents an example of an ambiguity diagram for the constant frequency pulse train. The contour plots in Figures A.13 and A.14 show that the results obtained agree with the theoretical ones previously defined. This can also be observed in Figures A.15 and A.16, which represent the time and frequency profiles, respectively. The time profile of the central pulse is a triangle and the frequency profile is a sinc function, as expected.

73
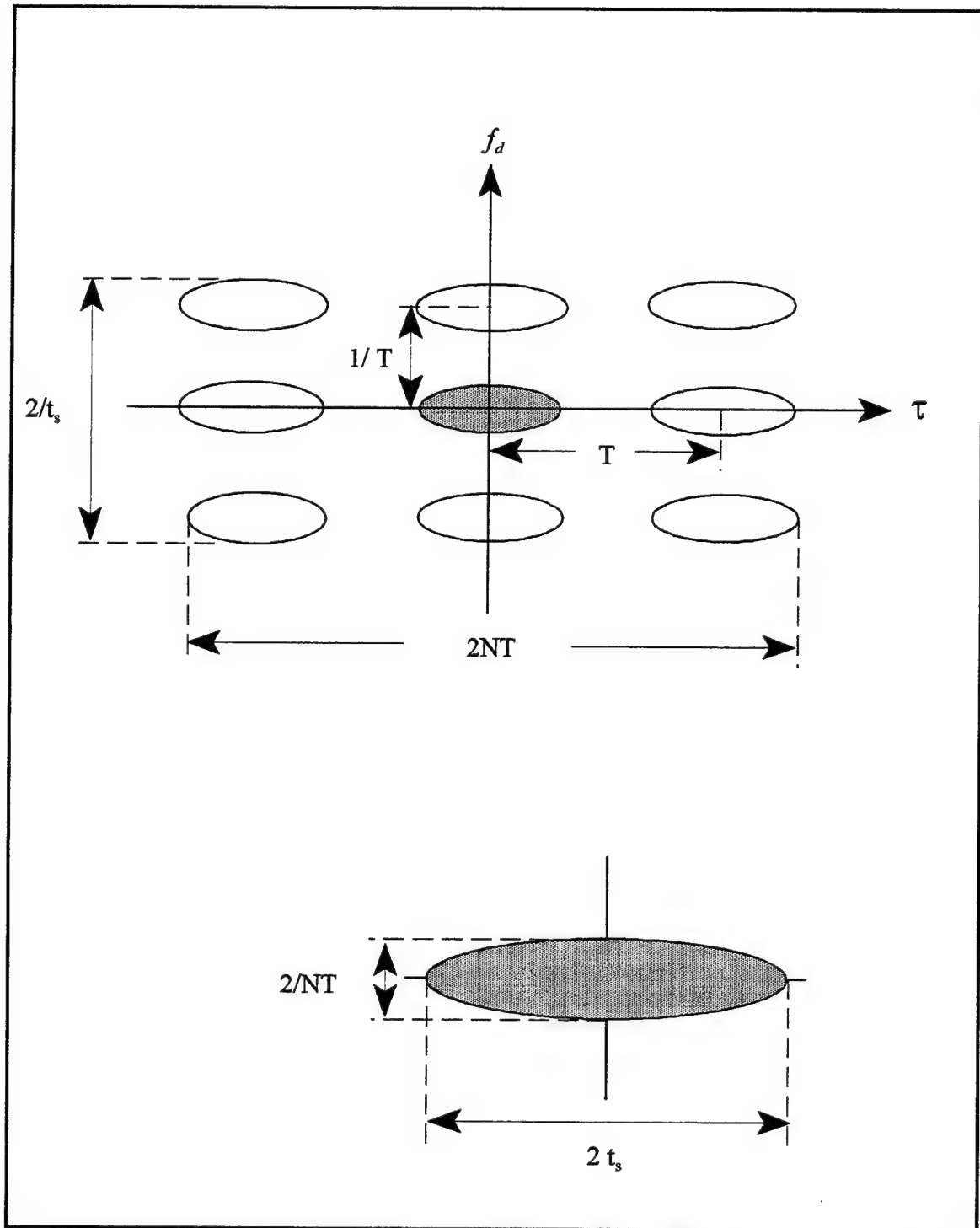
Figure A.11. Level contour of the ambiguity surface of a constant frequency pulse train.
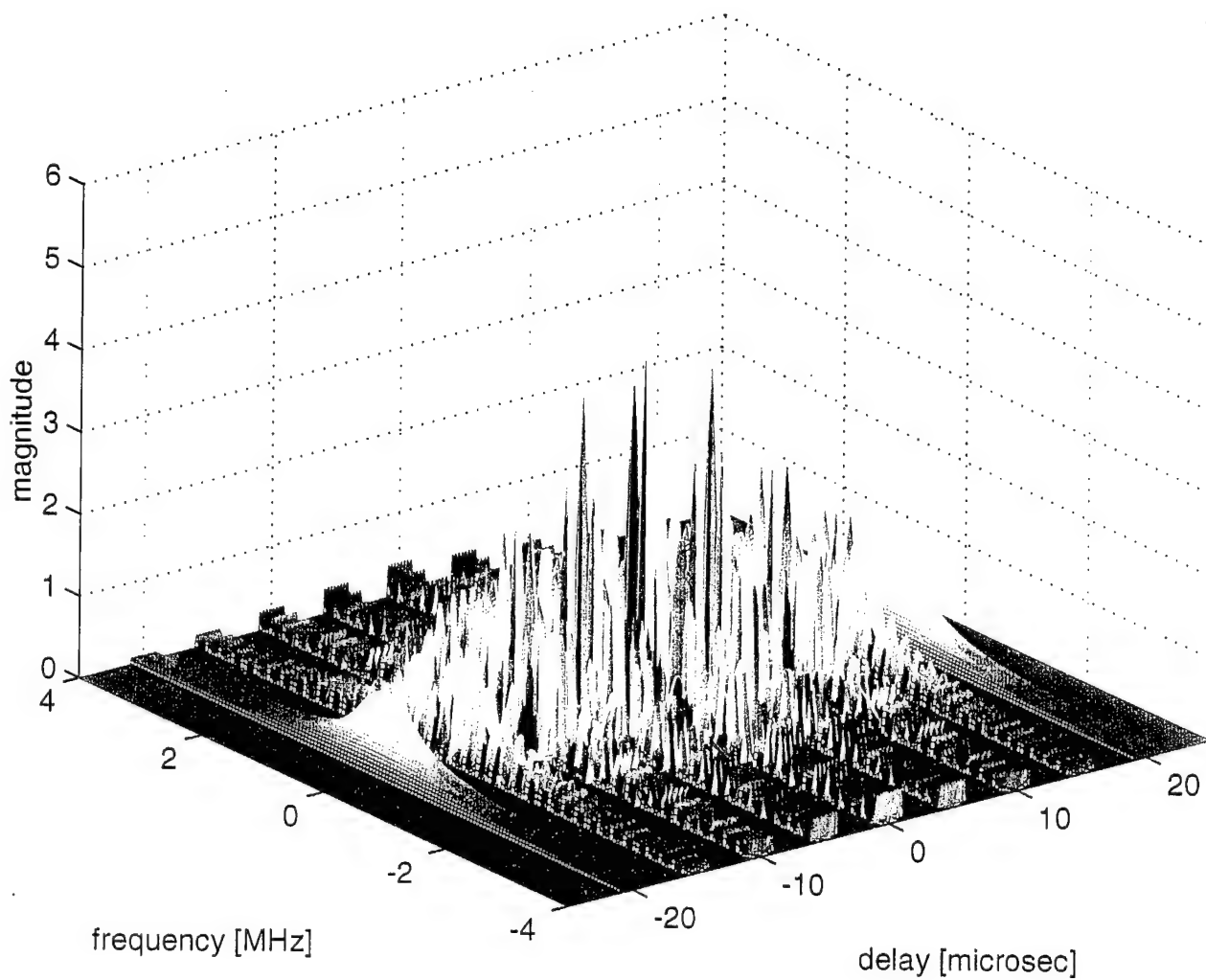
Figure A12.   Ambiguity diagram of a constant frequency pulse train.
(N=5, pulse width=1 microsec, PRI=5 microsec, Δf=0)

(a)

(b)
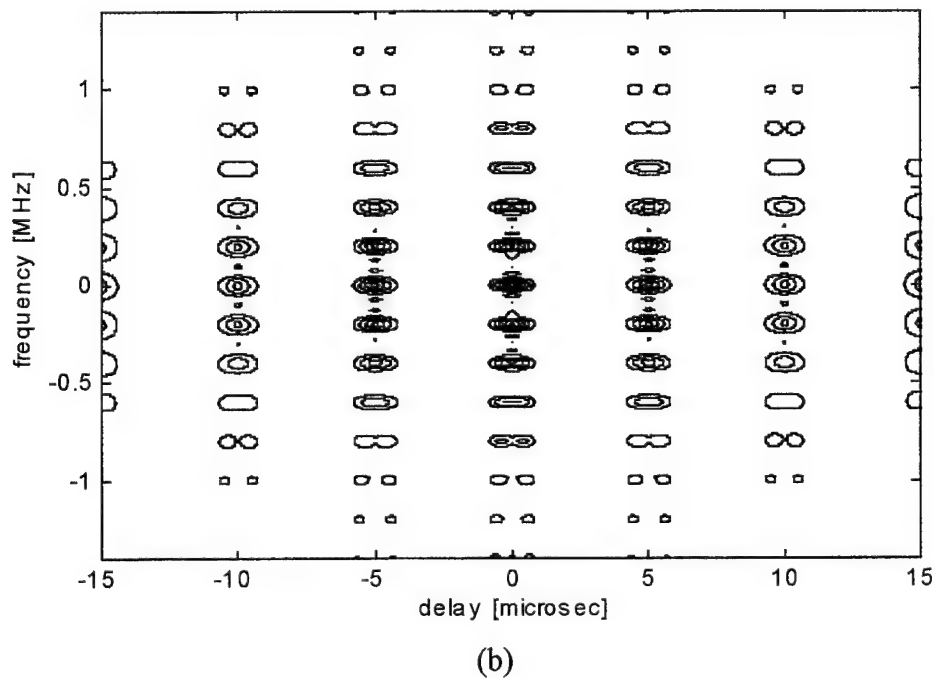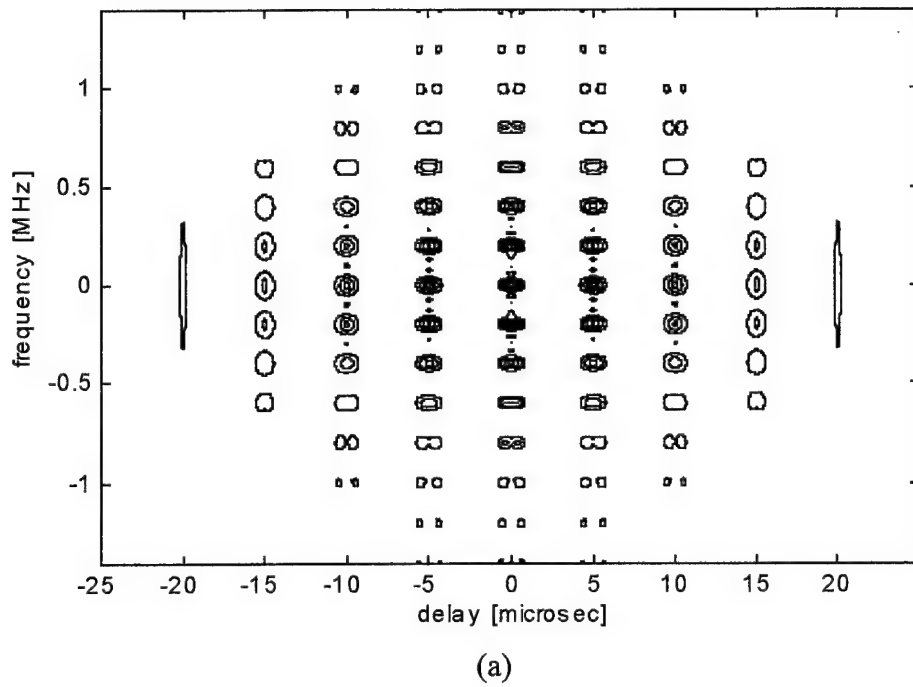
Figure A.13. Contour plots of the ambiguity diagram of a constant frequency pulse
train (N=5, pulse width=1 microsec, PRI=5 microsec, Δf=0)
(a) Global view.
(b) Magnified view.

Figure A.14.   Contour plots of the ambiguity diagram of a constant frequency pulse
train. (N=5, pulse width =1 microsec, PRI=5 microsec, Δf=0)
(a) Magnified view.
(b) Magnified view of the central peak.
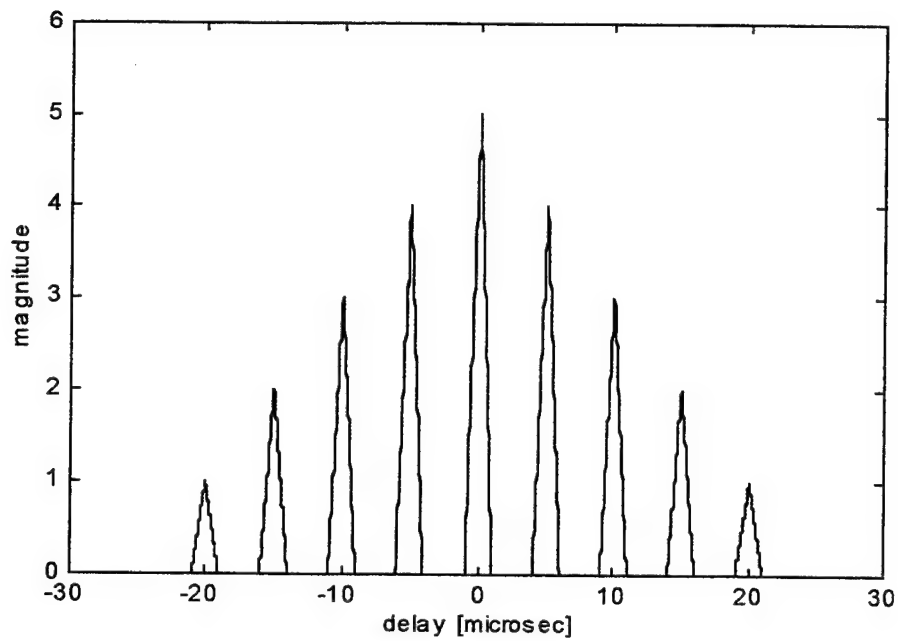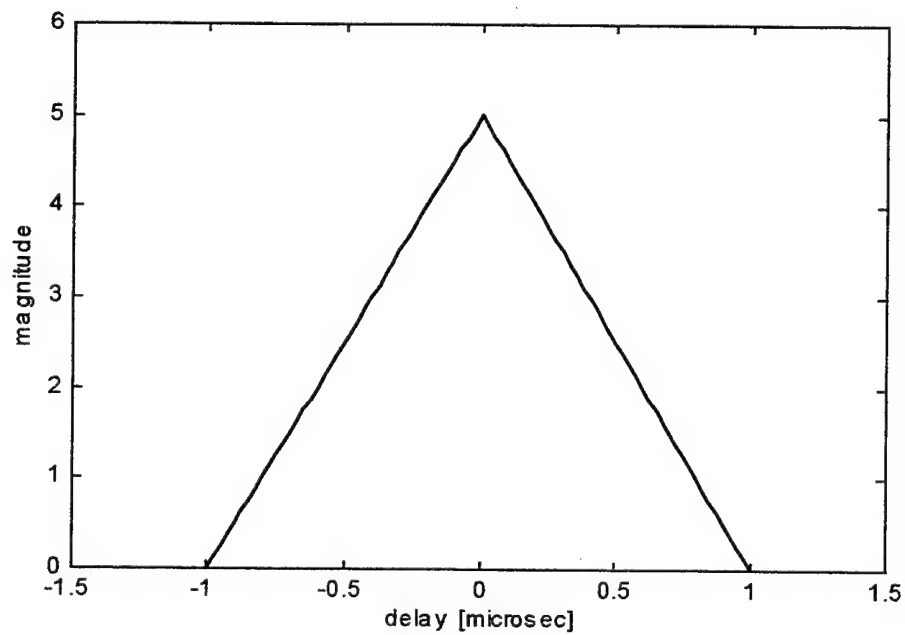
Figure A.15. Time profiles of the ambiguity diagram of a constant frequency pulse
train. (N=5, pulse width =1 microsec, PRI=5 microsec, $\Delta f=0$)
(a) Global view.
(b) Magnified view.
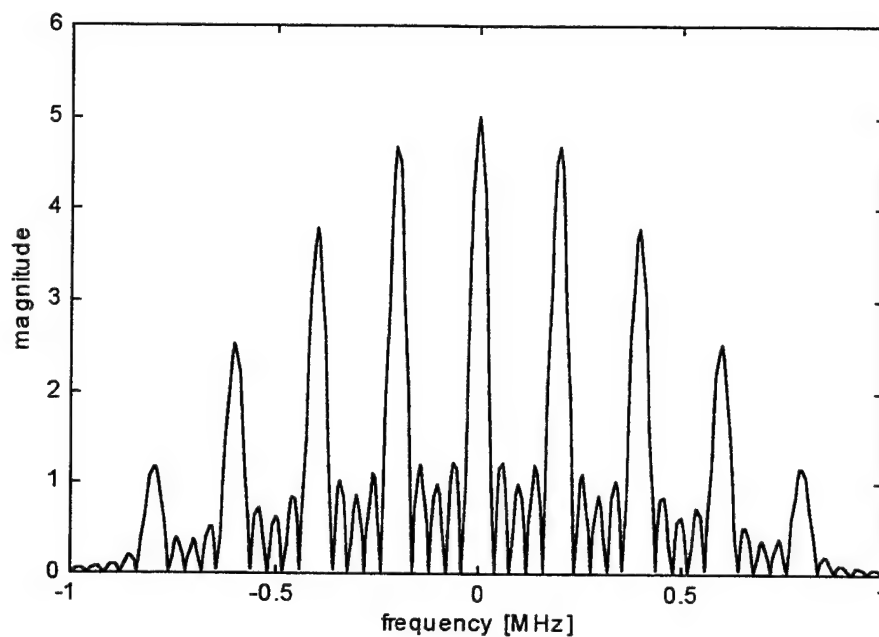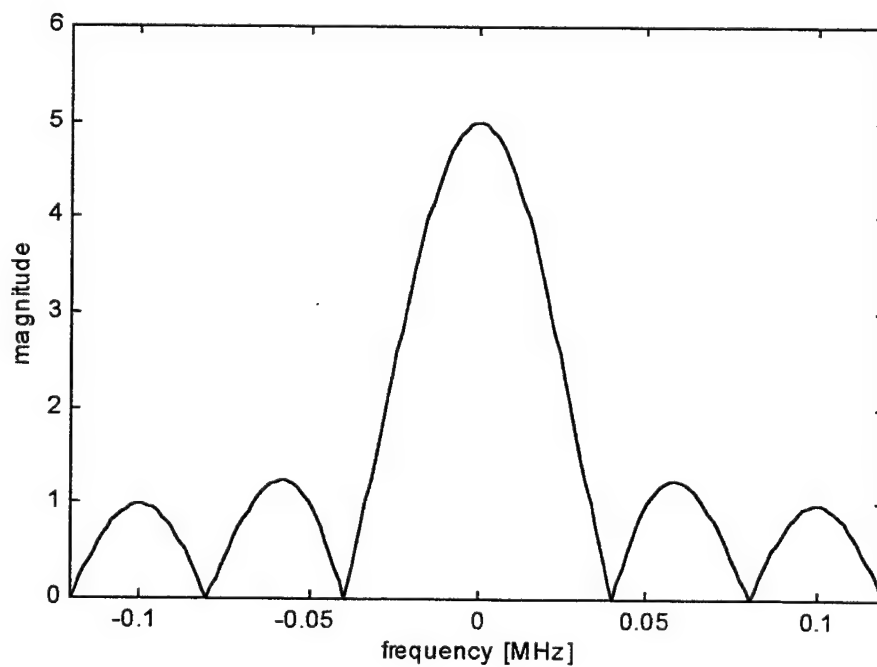
Figure A.16. Frequency profile of the ambiguity diagram of a constant frequency
pulse train . (N=5, pulse width =1 microsec, PRI=5 microsec, Δf=0)
(a) Global view.
(b) Magnified view.

APPENDIX B. MATLAB SOURCE CODES

```
% File name: program1.m
% Title: Plot generation
% Date of last revision: 4 Mar 1996
% Written by: Paulo A. Soares
% Comments: This program generates 3 plots for the SFWF design.
%***************************************************************************

clear
% ------------------- specifications ----------------------
vmin=150;vmax=1000;
f01=3e9;f02=5e9;f03=7e9;f04=10e9;
tot1=5e-3;tot2=10e-3;tot3=15e-3;tot4=20e-3;

% ---------------- computations & plots -----------------
c=3e8;
lambda1=c/f01;lambda2=c/f02;
lambda3=c/f03;lambda4=c/f04;

-% ----------------------- plot #1 -------------------------
dr=0.01:0.01:1;
fr1=(dr.\vmax)+((2/lambda1)*(vmax+vmin));
fr2=(dr.\vmax)+((2/lambda2)*(vmax+vmin));
fr3=(dr.\vmax)+((2/lambda3)*(vmax+vmin));
fr4=(dr.\vmax)+((2/lambda4)*(vmax+vmin));
figure(1)
  plot(dr,fr1/1e3,'w'),hold on
  plot(dr,fr2/1e3,'w'),hold on
  plot(dr,fr3/1e3,'w'),hold on
  plot(dr,fr4/1e3,'w')
  axis([0.01,1,10,110])
  xlabel('Range Resolution (meters)')
  ylabel('Minimum PRF (Khz)')
  text(0.75,27,'fo=3GHz'),text(0.75,42,'fo=5GHz')
  text(0.75,57,'fo=7GHz'),text(0.75,81,'fo=10GHz')
  text(0.2,100,'fo = nominal carrier frequency')

% ------------------------ plot #2 --------------------------
lambda=0.03:0.001:0.129;
k=(dr.\vmax);
fr1=(lambda.\2)*(vmax+vmin)+k;
N11=tot1*fr1;
N21=tot2*fr1;
N31=tot3*fr1;
figure(2)
  plot(fr1/1e3,N11,'w'),hold on
  plot(fr1/1e3,N21,'w'),hold on
  plot(fr1/1e3,N31,'w'),hold on
  axis([20,180,0,3000])
  xlabel('PRF (KHz)')
```

81

```
  ylabel('N')
  text(140,900,'tot=5ms'),text(140,1700,'tot=10ms')
  text(140,2550,'tot=15ms')
  text(50,2500,'tot = time-on-target')

% ------------------------plot #3------------------------
deltar1=0.3;
deltar2=0.5;
deltar3=1;
N=1:1:2048;
deltaf1=(2*N*deltar1*1e6).\c;
deltaf2=(2*N*deltar2*1e6).\c;
deltaf3=(2*N*deltar3*1e6).\c;
figure(3)
  plot(N,deltaf1,'w'),hold on
  plot(N,deltaf2,'w'),hold on
  plot(N,deltaf3,'w')
  axis([0,2100,0,1])
  xlabel('N')
  ylabel('Frequency Step (MHz)')
  text(1700,0.12,'dr=1m'),text(1700,0.21,'dr=0.5m'),text(1700,0.33,'dr=0.3m')
  text(1200,0.8,'dr = range resolution')
```

```
% Filename: program2.m
% Title: Main program for SFWF design
% Date of last revision: 28 Feb 1996
% Written by: Paulo A. Soares
% Comments: This program computes the exact design parameters frmin, df, N and tau, and then
%           rounds it in accordance with previously defined criteria.
%**************************************************************************

clear
c=3e8;Nmax=2048;
vmin=150;vmax=1000;
dr=input('  Enter the desired range resolution in meters : ');
while dr <= 0
  dr=input('  You must enter a positive value. Please try again : ')
end
f0=input('  Enter the nominal carrier frequency in GHz : ');
while f0 <= 0
  f0=input('  You must enter a positive value. Please try again : ')
end
lambda=c/(f0*1e9);
tot=input('  Enter the time-on-target in msec : ');
while tot <= 0
  tot=input('  You must enter a positive value. Please try again : ')
end
  frmin=(((2/lambda)*(vmax+vmin))+(vmax/dr))/1e3;
  fr=ceil(frmin);
while rem(fr,5) ~= 0
  fr=fr+1;
end
Nmin=ceil(tot*fr);
N=Nmin;
if N<=2
  N=2;
end
elseif N==3 | N==4
  N=4;
end
elseif N>4 & N<=9
  N=8;
end
elseif N>9 & N<=17
  N=16;
end
elseif N>17 & N<=34
  N=32;
end
elseif N>34 & N<=68
  N=64;
end
elseif N>68 & N<=136
  N=128;
end
elseif N>136 & N<=272
  N=256;
end
```

```
  elseif N>272 & N<=544
    N=512;
  end
  elseif N>544 & N<=1088
    N=1024;
  end
  elseif N>1088
    N=Nmax;
  end
  Nround=N;
  frround=Nround/tot;
  frround=ceil(frround);
  while rem(frround,5) ~=0
    frround=frround+1;
  end
  totround=Nround/frround;
  dfmin=c/(2*Nmin*dr*1e6);
  df=c/(2*Nround*dr*1e6);
  stepsizedf=0.2;
  dfround=ceil(df/stepsizedf);
  dfround=dfround*stepsizedf;
  taumin=(2*vmin)/(lambda*dfmin*frmin);
  tau=(2*vmin)/(lambda*dfround*frround);
  stepsizetau=10;
  tauround=ceil(tau/stepsizetau);
  tauround=tauround*stepsizetau;
  acdr=(c/(2*Nround*dfround))*1e-6;
  stepsizeacdr=0.01;
  acdrround=ceil(acdr/stepsizeacdr);
  acdrround=acdrround*stepsizeacdr;
  fprintf('\n The calculated design parameters are:\n')
  fprintf('   (minimum values in brackets)\n\n')
  fprintf('   -PRF = %3.2f KHz            (%3.2f KHz)\n',frround,frmin);
  fprintf('   -Frequency step = %3.2f MHz        (%3.2f MHz)\n',dfround,dfmin);
  fprintf('   -Pulse width = %3.2f nsec      (%3.2f nsec)\n',tauround,taumin);
  fprintf('   -Number of pulses = %4.0f          (%4.0f)\n',Nround,Nmin);
  fprintf('   -Actual range resolution = %3.2f m\n',acdrround);
  fprintf('   -Actual time-on-target = %3.2f msec ',totround);
```

84

```
% Filename: program3.m
% Title: Ambiguity function of the simple pulse by correlation method
% Date of last revision: 6 Apr 1996
% Written by: Paulo A. Soares
% Comments: This program draws four plots of the ambiguity function  for a single pulse.
%*********************************************************************************

clear;
tau=1;
nx=50;
ny=201;
t=[0:nx-1]*tau/nx;
dt=t(2)-t(1);
z=[];
fd=linspace(-10/tau,10/tau,ny);
u1=ones(1,nx);
for m=1:ny
 u2=u1.*exp(j*2*pi*fd(m)*t);
 c=xcorr(u2,u1).*dt;
 z=[z;abs(c)];
end
t=[fliplr(-t),t(2:nx)];
figure(1)
 mesh(t,fd,z),grid
 xlabel('delay [microsec]')
 ylabel('frequency [MHz]')
 zlabel('magnitude')
figure(2)
 contour(t,fd,z,7),grid
 xlabel('delay [microsec]')
 ylabel('frequency [MHz]')
figure(3)
 plot(t,z((ny+1)/2,:),'w')
 xlabel('delay [microsec]')
 ylabel('magnitude')
figure(4)
 plot(fd,z(:,nx),'w')
 xlabel('frequency [MHz]')
 ylabel('magnitude')
```

```
% Filename: program4.m
% Title: Ambiguity function of the LFM pulse by correlation method
% Date of last revision: 6 Apr 1996
% Written by: Paulo A. Soares
% Comments: This program draws four plots of the ambiguity function for a LFM pulse.
%*************************************************************************

clear;
tau=1;
mu=4;
nx=50;
ny=201;
t=[0:nx-1]*tau/nx;
dt=t(2)-t(1);
z=[];
fd=linspace(-10/tau,10/tau,ny);
for m=1:ny
  u1=exp(j*pi*mu.*t.*t);
  u2=conj(u1).*exp(j*2*pi*fd(m)*t);
  c=conv(u2,fliplr(u1)).*dt;
  z=[z;abs(c)];
end
t=[fliplr(-t),t(2:nx)];
figure(1)
  mesh(t,fd,z),grid
  xlabel('delay [microsec]')
  ylabel('frequency [MHz]')
  zlabel('magnitude')
figure(2)
  contour(t,fd,z,5),grid
  xlabel('delay [microsec]')
  ylabel('frequency [MHz]')
figure(3)
  plot(t,z((ny+1)/2,:),'w')
  xlabel('delay [microsec]')
  ylabel('magnitude')
figure(4)
  plot(fd,z(:,nx),'w')
  xlabel('frequency [MHz]')
  ylabel('magnitude')
```

86

```
% Filename: program5.m
% Title: Ambiguity function of the step frequency radar by the correlation method
% Date of last revision: 26 Apr 1996
% Written by: Paulo A. Soares
% Comments: This program computes and plots several figures of the ambiguity function of the
%              step frequency radar, using the correlation method.
%*****************************************************************************


%-------------------------------------------------------------------------------------------------
%                                    Parameters initialization
%-------------------------------------------------------------------------------------------------
clear;                           % clears all variables
tau=1;                           % tau=pulse width
T=5;                             % T=period or pulse repetition interval (PRI)
N=10;                            % N=number of pulses
df=1;                            % df=frequency step
sampfreq=40;                     % sampfreq=sampling frequency
NT=N*T;                          % NT=total period of the waveform
nsamptau=sampfreq*tau;           % nsamptau=number of samples in one pulse width
nsampt0=sampfreq*(T-tau);        % nsampt0=number of samples in the interpulse period
nsamptau=floor(nsamptau);
nsampt0=floor(nsampt0);
nsampT=nsamptau+nsampt0;         % nsampT=number of samples in one PRI


%-------------------------------------------------------------------------------------------------
%                                    Definition of axis and resolution
%-------------------------------------------------------------------------------------------------
P=[ones(1,nsamptau),zeros(1,nsampt0)];
t=linspace(0,NT,N*nsampT);             % time axis definition
ny=301;                                % number of points in the freq. axis
fd=linspace(-5/T,5/T,ny);              % freq. axis definition
dt=t(2)-t(1);                          % dt=time interval


%-------------------------------------------------------------------------------------------------
%                                    Computations
%-------------------------------------------------------------------------------------------------
s=[];
m=1:1:N;
for n=1:N
  s=[s,exp(j*2*pi*(m(n)-1)*df*t(nsampT*(n-1)+1:nsampT*n)).*P];
end
z=[];
for L=1:ny
  f=fd(L);
  s1=conj(s).*exp(j*2*pi*f*t);
  s2=s;
  c=conv(s1,fliplr(s2)).*dt;
  %z=[z;(abs(c)).^2];
  z=[z;abs(c)];
end
[l,r]=size(z);
t=[fliplr(-t),t(2:N*nsampT);
```

87

```
%-------------------------------------------------------------------------------
%                        Plotting of the results and axis labeling
%-------------------------------------------------------------------------------
figure(1)
  mesh(t,fd,z),grid
  xlabel('delay [microsec]')
  ylabel('frequency [MHz]')
figure(2)
  contour(t,fd,z,5)
  axis([-10 10 -1 1])
  xlabel('delay [microsec]')
  ylabel('frequency [MHz]')
figure(3)
  plot(t,z((ny+1)/2,:))
  axis([-30 30 0 12])
  xlabel('delay [microsec]')
  ylabel('magnitude')
figure(4)
  plot(fd',z(:,(r+1)/2),'w')
  xlabel('frequency [MHz]')
  ylabel('magnitude')
figure(5)
  contour(t,fd,z,5)
  axis([-1.5 1.5 -0.2 0.2])
  xlabel('delay [microsec]')
  ylabel('frequency [MHz]')
figure(6)
  plot(t,z((ny+1)/2,:))
  axis([-1.5 1.5 0 12])
  xlabel('delay [microsec]')
  ylabel('magnitude')
figure(7)
  plot(fd',z(:,(r+1)/2)')
  xlabel('frequency [MHz]')
  axis([-0.12 0.12 0 6])
```

```matlab
% Filename: program6.m
% Title: Ambiguity function of the step frequency radar by the equation method
% Date of last revision: 26 Apr 1996
% Written by: Paulo A. Soares
% Comments: This program computes and plots several figures of the ambiguity function of the
%           step frequency radar, using the equation method.
%**************************************************************************
%-------------------------------------------------------------------------
%                          Parameters initialization
%-------------------------------------------------------------------------
clear;                      % clears all variables
tau=1;                      % tau=pulse width
T=5;                        % T=pulse repetition interval (PRI)
N=10;                       % N=number of pulses
df=1;                       % df=frequency step
d=tau/T;                    % d=duty cycle


%-------------------------------------------------------------------------
%                          Definition of axis and resolution
%-------------------------------------------------------------------------
nx=101;                          % nx=number of points in the time axis
t=linspace(-N*T,N*T,nx);         % time axis definition
ny=3001;                         % ny=number of points in the freq. axis
fd=linspace(-5/T,5/T,ny);        % freq.axis definition
%-------------------------------------------------------------------------
%                          Computations
%-------------------------------------------------------------------------
p=floor(t/T);
r=(t/T)-p;
z=[];
for m=1:ny
x=[];
f=fd(m);
for n=1:nx
pp=p(n);
rr=r(n);
f1=f-pp*df;
f2=f-(2*pp+rr)*df;
f3=f-(pp+1)*df;
f4=f-(2*pp+rr+1)*df;
if rr>=0 & rr<d
 if f1==0
  x1=1;
 else
  x1=(sin(pi*f1*(tau-rr*T)))./(pi*f1*(tau-rr*T));
 end
 if rem(f2*T,1)==0
  x2=N-abs(pp);
 else
  x2=(sin(pi*f2*(N-abs(pp))*T))./(sin(pi*f2*T));
 end
 x=[x,(tau-rr*T).*x1*x2];
elseif rr<1 & rr>=(1-d)
 if f3==0
  x1=1;
```

89

```
    else
      x1=(sin(pi*f3*(tau+(rr-1)*T)))./(pi*f3*(tau+(rr-1)*T));
    end
    if rem(f4*T,1)==0
      x2=N-abs(pp+1);
    else
      x2=(sin(pi*f4*(N-abs(pp+1))*T))./(sin(pi*f4*T));
    end
    x=[x,(tau+(rr-1)*T).*x1*x2];
  else
    x=[x,0];
  end
end
z=[z;x];
end
z=abs(z);


%------------------------------------------------------------------------------------------
%                          Plotting of results and axis labeling
%------------------------------------------------------------------------------------------
figure(1)
  mesh(t,fd,z),grid
  xlabel('delay [microsec]')
  ylabel('frequency [MHz]')
figure(2)
  contour(t,fd,z,5)
  axis([-6 6 -0.2 0.2])
  xlabel('delay [microsec]')
  ylabel('frequency [MHz]')
figure(3)
  plot(t,z((ny+1)/2,:))
  xlabel('delay [microsec]')
  ylabel('magnitude')
figure(4)
  plot(fd',z(:,(nx+1)/2)')
  xlabel('frequency [MHz]')
  ylabel('magnitude')
figure(5)
  contour(t,fd,z,5')
  axis([-0.7 0.7 -0.05 0.05])
  xlabel('delay [microsec]')
  ylabel('frequency [MHz]')
figure(6)
  plot(t,z((ny+1)/2,:))
  axis([-1.5 1.5 0 12])
  xlabel('delay [microsec]')
  ylabel('magnitude')
figure(7)
  plot(fd',z(:,(nx+1)/2)')
  axis([-0.05 0.05 0 0.5])
  xlabel('frequency [MHz]')
  ylabel('magnitude')
```

LIST OF REFERENCES

1.   Merill I. Skolnik, *Introduction to Radar Systems*, Second Edition, McGraw-Hill, Inc., 1980.

2.   Donald R. Wehner, *High Resolution Radar*, Second Edition, Artech House Inc., 1995.

3.   Byron Edde, *Radar. Principles,Technology, Applications*, Prentice-Hall, Inc., 1993.

4.   George W. Stimson, *Introduction to Airborne Radar*, Hughes Aircraft Company, 1983.

5.   Nicholas C. Currie, *Radar Reflectivity Measurement: Techniques & Applications*, Artech House, Inc., 1989.

6.   James A. Scheer, and James L. Kurtz, *Coherent Radar Performance Estimation*, Artech House Inc., 1993.

7.   Nadav Levanon, *Radar Principles*, Wiley & Sons, Inc., 1988.

INITIAL DISTRIBUTION LIST

No. Copies

1. Defense Technical Information Center   2
   8725 John J. Kingman Rd., STE 0944
   Ft. Belvoir, VA 22060-6218

2. Dudley Knox Library   2
   Code 52
   Naval Postgraduate School
   Monterey, CA 93943-5101

3. Chairman, Code EC   1
   Department of Electrical and Computer Engineering
   Naval Postgraduate School
   Monterey, CA 93943-5121

4. Professor G. S. Gill, Code EC/Gl   5
   Department of Electrical and Computer Engineering
   Naval Postgraduate School
   Monterey, CA 93943-5121

5. Thomas E. Tice, Code 755   1
   NCCOSC, NRad
   71 Catalina Blvd.
   San Diego, CA 92152-5000

6. William Miceli   1
   Office of Naval Research
   Attn: ONR313
   Ballston Tower 2
   800 N. Quincey St.
   Arlington, VA 22217-5660

7. James Hall   1
   Office of Naval Research
   Attn: ONR313
   Ballston Tower 2
   800 N. Quincey St.
   Arlington, VA 22217-5660